

Supplementary Information

An erythrocyte-delivered photoactivatable oxaliplatin nanoprodruq for enhanced antitumor efficacy and immune response

Na Wang,^a ‡ Zhiqin Deng,^{a,g} ‡ Qi Zhu,^c ‡ Jianxiong Zhao,^c Kai Xie,^f Peng Shi,^f Zhigang Wang,^e Xianfeng Chen,^d Feng Wang,^{c,g} Jiahai Shi,^b and Guangyu Zhu^{a,g,}*

^aDepartment of Chemistry, City University of Hong Kong, Hong Kong SAR, P. R. China

^bDepartment of Biomedical Sciences, City University of Hong Kong, Hong Kong SAR, P. R. China

^cDepartment of Materials Science and Engineering, City University of Hong Kong, Hong Kong SAR, P. R. China

^dSchool of Engineering, Institute for Bioengineering, The University of Edinburgh, Mayfield Road, Edinburgh EH9 3JL, United Kingdom

^eSchool of Pharmaceutical Sciences, Health Science Center, Shenzhen University, Shenzhen 518060, P. R. China

^fDepartment of Biomedical Engineering, City University of Hong Kong, Hong Kong SAR, P. R. China

^gCity University of Hong Kong Shenzhen Research Institute, Shenzhen 518057, P. R. China

‡These authors contributed equally to this work.

*Correspondence: guangzhu@cityu.edu.hk

Table of Contents

Experimental Details.....	S1
Materials and Instruments.....	S1
Synthesis of PPA-Pt ^{IV} -COOH.....	S2
Synthesis of NH ₂ -NCs.....	S2
Quantification of Amine Moieties on NH ₂ -NCs.....	S3
Loading of PPA-Pt ^{IV} -COOH on NH ₂ -NCs.....	S3
Characterizations of Modified NCs.....	S4
Release of Pt from PPA-Pt ^{IV} -NCs.....	S4
Detection of Singlet Oxygen.....	S4
Cell Lines and Cell Culture Conditions.....	S4
Time-dependent Cellular Accumulation of Pt.....	S5
Photocytotoxicity of PPA-Pt ^{IV} -NCs with or without Irradiation in Different Cell Lines.....	S5
Concentration-dependent Cellular Accumulation of Pt in A2780cisR Cells.....	S5
Pt Level in Genomic DNA with or without Irradiation.....	S5
Intracellular ROS Detection.....	S6
PEGylation of PPA-Pt ^{IV} -NCs.....	S6
Synthesis of ERY ₁ -PEG _{3k} /PPA-Pt ^{IV} -NCs.....	S6
Stability of PPA-Pt ^{IV} -COOH, PPA-Pt ^{IV} -NCs, and ERY ₁ -PEG _{3k} /PPA-Pt ^{IV} -NCs in Fresh Mouse Whole Blood....	S7
Blood Collection and Preparation of Erythrocytes Binding <i>In Vitro</i>	S8
Confocal Imaging Assessment for Erythrocytes Binding.....	S8
Sample Preparation for Scanning Electron Microscope (SEM).....	S8
Flow Cytometry for Erythrocyte Binding Assessment.....	S9
Flow Cytometry for Erythrocyte Binding Assessment with GYPA Antibody.....	S9
ICP-OES to Detect Conjugated Pt on Erythrocyte.....	S9
Maximum Tolerated Dose of ERY ₁ -PEG _{3k} /PPA-Pt ^{IV} -NCs <i>In Vivo</i>	S9
Pharmacokinetic Test <i>In Vivo</i>	S10
Bioimaging and Biodistribution <i>In Vivo</i>	S10
Anticancer Evaluation in 4T1 Xenograft Model.....	S11
T Cell Measurement in Tumor by Flow Cytometry.....	S12
Histology.....	S12
Blood Biochemistry Measurement.....	S12

Animal Ethics	S13
Statistics Analysis	S13
Results	S14
Fig. S1 TEM images of core, core-shell, core-shell-shell NCs with OA ligand (OA-NCs), bare core-shell-shell NCs (bare NCs), and core-shell-shell NCs covered with PEI (PEI-NCs)	S14
Fig. S2 FT-IR spectra of OA-NCs, bare NCs, and PEI-NCs	S15
Fig. S3 UV absorbance spectra of sample solution and standard solutions containing different concentrations of Fmoc and standard curve of various concentrations of Fmoc and the sample solution at $\lambda = 301$ nm	S16
Fig. S4 Chemical structure of PPA-Pt ^{IV} -COOH.....	S17
Fig. S5 RP-HPLC (420 nm) chromatograms of PPA-Pt ^{IV} -COOH stock solution	S17
Fig. S6 ¹ H NMR of PPA-Pt ^{IV} -COOH	S18
Fig. S7 ¹³ C NMR of PPA-Pt ^{IV} -COOH	S19
Fig. S8 ¹⁹⁵ Pt NMR of PPA-Pt ^{IV} -COOH.....	S20
Fig. S9 The photoactivation property of PPA-Pt ^{IV} -COOH tested through HPLC at 220 nm..	S21
Fig. S10. TEM images of A) PPA-Pt ^{IV} -NCs (4%, w/w), B) PPA-Pt ^{IV} -NCs (18%, w/w), and C) PPA-Pt ^{IV} -NCs (22%, w/w)	S22
Fig. S11 FT-IR spectra of PEI-NCs, PPA-Pt ^{IV} -NCs, PPA-Pt ^{IV} -NCs, PEG _{3k} /PPA-Pt ^{IV} -NCs, and ERY ₁ -PEG _{3k} /PPA-Pt ^{IV} -NCs	S23
Fig. S12 Release of Pt from PPA-Pt ^{IV} -NCs (0.1 mg/mL) with or without irradiation in PBS containing 0.5 mM ascorbate (pH 7.4) and the release of oxaliplatin after irradiation was confirmed by electrospray ionization mass spectrometry (ESI-MS)	S24
Fig. S13 Generation of ¹ O ₂ through DPBF assay	S25
Fig. S14 Time-dependent cellular accumulation of Pt in various cell lines after treated with PPA-Pt ^{IV} -NCs (0.1 mg/mL NCs) for 1, 2, 4, and 6 h	S26
Fig. S15 Phototoxicity of PPA-Pt ^{IV} -COOH in 4T1, MCF-7, A2780, A2780cisR, and MRC-5 cells with or without 808 nm irradiation.	S26
Fig. S16 Phototoxicity of PPA-Pt ^{IV} -COOH in 4T1, MCF-7, A2780, A2780cisR, and MRC-5 cells with or without 660 nm irradiation	S26
Fig. S17 Concentration-dependent cellular accumulation of Pt in A2780cisR cells	S299
Fig. S18 Pt levels of genomic DNA in A2780cisR cells	S30
Fig. S19 Confocal images of H ₂ DCFDA-stained HeLa cells treated with 3 mM H ₂ O ₂ for 15 min or 100 μ g mL ⁻¹ PPA-Pt ^{IV} -NCs for 1 h with or without 808 nm laser irradiation afterward	S31
Fig. S20 Phototoxicity of ERY ₁ -PEG _{3k} /PPA-Pt ^{IV} -NCs in 4T1, MCF-7, A2780, A2780cisR, and MRC-5 cells with or without 808 nm irradiation.....	S32
Fig. S21 SEM images of erythrocytes incubated with 5 mg/mL BSA as control, PEG _{3k} /PPA-Pt ^{IV} -NCs, and ERY ₁ -PEG _{3k} /PPA-Pt ^{IV} -NCs overnight at 4 °C in the dark.....	S33

Fig. S22 Confocal fluorescence microscopy images of erythrocytes incubated with various complexes overnight at 4 °C in the dark	S34
Fig. S23 A quantitative analysis of fluorescence histogram by flow cytometry depicting the erythrocytes and after incubated with indicated complexes (PEG _{3k} /PPA-Pt ^{IV} -NCs, and ERY ₁ -PEG _{3k} /PPA-Pt ^{IV} -NCs)	S35
Fig. S24 Merged flow cytometry depicting the fluorescence intensity of erythrocytes incubated with indicated complexes	S35
Fig. S25 A quantitative analysis of fluorescence histogram by flow cytometry depicting the glycophorin A (GYPA) on erythrocytes and after incubated with indicated complexes (PEG _{3k} /PPA-Pt ^{IV} -NCs, and ERY ₁ -PEG _{3k} /PPA-Pt ^{IV} -NCs)	S36
Fig. S26 Pt levels on erythrocytes	S37
Fig. S27 The change of body weight in various doses of ERY ₁ -PEG _{3k} /PPA-Pt ^{IV} -NCs for MTD test (<i>i.v.</i> injection, single dose on Day 0)	S38
Fig. S28 <i>In vivo</i> fluorescence imaging of 4T1 tumor-bearing BALB/c mice and corresponding organs after intravenously (<i>i.v.</i>) injected with various complexes at 5 min, 3 h, 17 h, and 24 h post-injection	S39
Fig. S29 The schedule of <i>in vivo</i> experiment to evaluate the anticancer activity in the 4T1 xenograft model	S40
Fig. S30 The digital photos on Day 1 of the 4T1 xenograft model after different treatments.....	S41
Fig. S31 The digital photos on Day 14 of the 4T1 xenograft model after different treatments.....	S42
Fig. S32 The digital photos of the same mouse from ERY ₁ -PEG _{3k} /PPA-Pt ^{IV} -NCs group with 7 times of 808 nm irradiation	S43
Fig. S33 The change of body weight of the 4T1 xenograft model with different treatments.....	S44
Fig. S34 Spleen weights of different groups of 4T1 xenograft model after the experiment terminated .	S45
Fig. S35 Hematology study of blood plasma from 4T1 xenograft model after experiment terminated (Day 14) with aspartate transaminase (AST), alanine aminotransferase (ALT), creatinine, blood urea nitrogen (BUN), and uric acid (UA)	S46
Fig. 36 H&E staining of the organs and tumors at the end of antitumor studies	S47
Table S1. Diameter and zeta potential of PEI-NCs and the various nanocomplexes containing Pt(IV) prodrug	S48
Table S2. Calculated pharmacokinetics parameters	S49
Supplementary References	S50

Experimental Details

Materials and Instruments

Pyropheophorbide a (PPA) was obtained from Arethusa Life Sciences Co., LTD. (Shanghai, China), and oxaliplatin was bought from Boyuan Technology (Shandong, China). 9-Fluorenylmethoxycarbonyl chloride (Fmoc-Cl), 1,3-diphenylisobenzofuran (DPBF), O-[N-(6-maleimidohexanoyl)aminoethyl]-O'-[3-(N-succinimidylxy)-3-oxopropyl]polyethylene glycol 3,000 (NHS-PEG_{3k}-MAL), N-(3-dimethylaminopropyl)-N'-ethylcarbodiimide hydrochloride (EDC), N-hydroxysuccinimide (NHS), poly-L-lysine solution (0.1%, w/v, in H₂O), yttrium(III) acetate hydrate (Y(CH₃CO₂)₃·xH₂O, 99.9% metals basis), ytterbium(III) acetate hydrate (Yb(CH₃CO₂)₃·xH₂O, 99.95% trace metals basis), neodymium(III) acetate hydrate (Nd(CH₃CO₂)₃·xH₂O, 99.9%), erbium(III) acetate hydrate (Er(CH₃CO₂)₃·xH₂O, 99.9% trace metals basis), sodium hydroxide (>98%), ammonium fluoride (>98%), 1-octadecene (ODE, 90%), oleic acid (OA, 90%), oleylamine (90%) were purchased from Sigma-Aldrich. Absolute ethanol (99.85%), methyl alcohol (99.99%), and cyclohexane (99.9%) were purchased from VWR International. 2',7'-dichlorodihydrofluorescein diacetate (H₂DCFDA), Dulbecco's Modified Eagle Medium (DMEM), Roswell Park Memorial Institute 1640 (RPMI 1640) medium, minimum essential medium (MEM), trypsin, phosphate buffered saline (PBS), fetal bovine serum (FBS), non-essential amino acids (NEAA), penicillin-streptomycin, sodium pyruvate, 3-(4,5-dimethyl-2-thiazolyl)-2,5-diphenyl-2H-tetrazolium bromide (MTT) were purchased from the Life Technologies. Bovine Serum Albumin (BSA) lyophilized powder was purchased from Acros Organics. Polyethylenimine (PEI, branched, MW 1200, 99%) solution was bought from International Laboratory USA. ERY₁ peptide (WMVLPWLPGLDGGSGCRG) was obtained from GL Biochem (Shanghai, China). Alexa Fluor® 488 conjugated glycophorin A polyclonal antibody (Cat# bs-2575R-A488) was purchased from Bioss antibodies USA. CD3 monoclonal antibody (17A2), FITC, eBioscience (Cat# 11-0032-80), CD4 monoclonal antibody (GK1.5), APC, eBioscience (Cat# 17-0041-82), CD8a monoclonal antibody (53-6.7), PE, eBioscience (Cat# 12-0081-82), and erythrocyte lysis buffer (1×), eBioscience (Cat# 00-4333-57) were obtained from Invitrogen, Thermo Fisher. All commercial products were applied as received without further purification. Flow cytometry experiments were performed on a CytoFLEX S Flow Cytometer (Beckman). NMR spectra were collected on a Bruker Ascend AVANCE III 600 MHz spectrometer. Chemical shifts were reported in parts per million relatives to residual solvent peaks. ESI-MS data were obtained on an Agilent API-150EX MS system. Analytical reversed-phase High-Performance Liquid Chromatography (RP-HPLC) was conducted on a Shimadzu Prominence LC-20AT HPLC system equipped with a reversed-phase C18 column (Phenomenex Garmin 250 × 4.60 mm, 5 μm, 110 Å). Unless indicated, test samples were monitored by UV absorbance at 420 nm: Solvent A (H₂O with 5% acetonitrile and 0.1% TFA) and solvent B (acetonitrile with 5% H₂O and 0.1% TFA) were used for a gradient elution at a flow rate of 1.0 mL/min. The test samples were eluted by using a program as follows: 0% B (0 min) → 20% B (7 min) → 100% B (12 min) → 100% B (25 min) → 0% B (27 min) → 0% B (30 min). Animal imaging was performed on a Bruker In-Vivo Xtreme II small animal imaging system.

Synthesis of PPA-Pt^{IV}-COOH

N-hydroxysuccinimide (NHS, 15 mg, 0.13 mmol) and 1-ethyl-3-(3-dimethylaminopropyl) carbodiimide hydrochloride (EDC, 30 mg, 0.15 mmol) in DMSO (3 mL) was added to get a mixture with pyropheophorbide a (PPA, 50 mg, 0.093 mmol). The reaction mixture was stirred overnight at room temperature, and then the resultant solution was added to ice-cold deionized (DI) water (30 mL) dropwise. The precipitate was collected by centrifugation and washed twice by ice-cold water. The precipitate was further lyophilized and redissolved in DMSO (3 mL). Pt(DACH)(OH)₂(ox) (40 mg, 0.093 mmol) was added to the solution, and the mixture was stirred at 60 °C overnight. The resultant solution was added to ice-cold DI water (30 mL) dropwise. The obtained precipitate was collected by centrifugation and washed twice by ice-cold DI water. The final precipitate was lyophilized to get the raw product, which was further purified by silica gel column chromatography using MeOH/CH₂Cl₂ (1:10) as an eluent to afford the target compound as a black powder. Yield: 49%. ¹H NMR (600 MHz, DMSO-d₆): 11.73 (1H, s), 9.43 (1H, s), 9.16 (1H, s), 8.84 (1H, s), 8.48-8.03 (5H, m), 6.28 (1H, d), 6.13 (1H, d), 5.15 (1H, d), 4.53 (1H, d), 4.25 (1H, d), 3.48 (3H, s), 3.47-3.41 (2H, m), 3.37 (3H, s), 3.01 (3H, s), 2.62 (4H, m), 2.41 (3H, m), 2.09 (2H, s), 1.75 (1H, s), 1.52 (1H, t), 1.42 (1H, m), 1.08 (1H, m). ¹³C NMR (151 MHz, DMSO-d₆): 195.8, 180.9, 180.1, 174.2, 174.0, 172.6, 163.9, 161.9, 154.4, 150.3, 148.3, 145.0, 141.1, 137.5, 136.2, 135.3, 132.2, 130.4, 129.4, 128.2, 123.2, 106.4, 104.4, 96.8, 94.2, 61.5, 51.6, 49.7, 47.9, 40.89, 33.41, 31.4, 31.3, 31.0, 30.7, 30.1, 24.0, 23.9, 23.3, 18.9, 17.8, 12.4, 12.0, 11.2. ¹⁹⁵Pt NMR (129 MHz, DMSO-d₆): 1610.96 (s). ESI-MS, [M+H]⁺: Found=1048.0; Calc.=1048.2.

Synthesis of NH₂-NCs

NH₂-NCs were synthesized following published protocols.^{1,2} Before covered with amine moieties, the dielectric NaYbF₄:Er@NaYF₄:Yb/Nd@NaYF₄:Ca nanocrystals were first synthesized.¹ The synthesis of core nanoparticles. Typically, 4 mL of Yb(CH₃CO₂)₃·xH₂O and Er(CH₃CO₂)₃·xH₂O aqueous solution (0.2 M) were added into a 50 mL round-bottom flask. Then 8 mL of oleic acid (OA), 2 mL oleylamine, and 10 mL of 1-octadecene (ODE) were added into the flask under stirring. The flask was raised to 125 °C to remove the water in the mixture and then raise the temperature to 175 °C for 60 min followed by cooling down to 45 °C. After that, 8 mL NH₄F (0.4 M) and 2 mL NaOH (1 M) in methanol solution were added into the flask and stirred for at least 2 h. The mixture was then heated to 110 °C followed by vacuuming and filling the argon. Then the temperature was adjusted to 285 °C in an argon atmosphere for 90 min, followed by cooling down to the room temperature. The synthesized core nanoparticles were collected by addition of ethanol and centrifugation at 6000 rpm for 3 min. The obtained product was washed with ethanol for 3 times and re-dispersed in cyclohexane.

The core-shell nanoparticles were further synthesized as below. The as-prepared core nanoparticles were used as seeds for the epitaxial growth of the shell layer. In a typical experiment, 4 mL of Y(CH₃CO₂)₃·xH₂O, Yb(CH₃CO₂)₃·xH₂O, and Nd(CH₃CO₂)₃·xH₂O aqueous solution (0.2 M) along with 8 mL of OA and 12 mL of ODE were added into a 50 mL flask and heated to 175 °C for 60 min under stirring. Then the flask was cooled down to 45 °C, followed by injection of 8 mL NH₄F (0.4 M) and 2 mL NaOH (1 M) in methanol as well as 4 mL cyclohexane dispersion of the core nanoparticles. After being stirred for 120 min, the mixture was then heated to 110 °C

followed by vacuuming and filling argon. Then, the flask was heated to 285 °C in an argon atmosphere for 90 min with constant stirring. After cooling down to room temperature, the products were collected, washed, and re-dispersed in cyclohexane.

The core-shell-shell NCs were prepared as following procedures. The synthetic process of the core-shell-shell nanocrystals was the same as that for the core-shell nanoparticles, except that $Y(CH_3CO_2)_3 \cdot xH_2O$ and $Ca(CH_3CO_2)_2 \cdot xH_2O$ were used as shell precursor and pre-synthesized core-shell nanoparticles were used as seeds.

Synthesis of ligand-free NCs. 4 mL prepared core-shell-shell nanocrystals were precipitated with ethyl alcohol and centrifugation at 6,000 rpm for 1 min. The organic solvent was removed and 8 mL 0.1 M HCl was added to form turbid liquid, followed by stewing for 24 h. Then the ligand-free particles were collected by removing the supernatant ligand and centrifugation at 14,000 rpm for 15 min.

Synthesis of PEI coated-NCs. 47.5 mg polyethylenimine (PEI) in 9.5 mL DI water was added into 20 mL sample bottle and the mixture was stirred for 30 min. 0.5 mL ligand-free nanoparticles were added into the PEI solution dropwise and the mixture was stirred for another 12 h. Then the PEI-coated nanoparticles were collected by centrifugation at 10,000 rpm for 15 min and re-dispersed in DI water, and stored in a fridge at 4 °C.

Quantification of Amine Moieties on NH₂-NCs

To quantitatively analyze amine moieties on NH₂-NCs, 9-fluorenylmethoxycarbonyl chloride (Fmoc-Cl) (9.1 mg, 3.5×10^{-5} mol) was added to 2 mL anhydrous DMF solution containing the dried NCs (0.4 mg).³ The mixture was stirred overnight for the reaction at room temperature. Then the solid was obtained after centrifugation (14,000 rpm, 30 min), and washed several times with methanol thoroughly. Precipitated NCs with Fmoc conjugation were dried under vacuum overnight. The lyophilized Fmoc-protected NCs were then precisely weighed and resuspended in 0.5 mL dimethylformamide (DMF). Then 0.1 mL piperidine was added to the Fmoc-conjugated NC solution for Fmoc cleavage by sonication for 20 min. The Fmoc cleaved NCs mixture was further centrifuged at 14,000 rpm for 20 min (Eppendorf), and the amine groups in the supernatant were quantified by Fmoc standard curve with UV absorption at $\lambda = 301$ nm.^{4,5}

Loading of PPA-Pt^{IV}-COOH on NH₂-NCs

PPA-Pt^{IV}-COOH was dissolved in DMF at a concentration of 8 mM (8.5 mg/mL). The NH₂-NCs (1 mg/mL) in water were well dispersed via ultrasonic and mixed with PPA-Pt^{IV}-COOH at the ratio of 0.07, 0.34, 0.68, 0.94, 1.41 (w/w, the ratio of PPA-Pt^{IV}-COOH to NH₂-NCs) in the presence of EDC/NHS (1.2 equivalent). After vigorously stirred overnight at room temperature in the dark, the synthesized PPA-Pt^{IV}-NCs were collected through centrifugation (14,000 rpm, 30 min), and washed three times with Milli-Q water to remove the free PPA-Pt^{IV}-COOH through centrifugation. PPA-Pt^{IV}-NCs were obtained with loading capacity of 3.9%, 15.3%, 22.6%, 22.9 %, 22.1% (wt%). The amount of Pt and Yb contents were quantified by inductively coupled plasma-optical emission spectrometry (ICP-OES, PerkinElmer Optima 8000). The loading capacity (LC wt%) is calculated by $LC \text{ wt\%} = m_1 / (m_0 + m_1)$, where m_0 is the mass of NCs, m_1 is the loaded mass of platinum(IV) prodrug. The synthesized PPA-Pt^{IV}-NCs were stored in 4 °C (in the dark) for further investigations and modifications.

Characterization of Modified NCs

The Pt content was determined by ICP-OES or inductively coupled plasma-mass spectrometry (ICP-MS, PerkinElmer). The UV-Vis spectrum was measured on a Shimadzu UV-1700 UV-vis spectrophotometer. Fourier transform infrared (FT-IR) measurements were performed on an FT-IR spectrophotometer (Nicolet iS50, USA). Transmission electron microscopy (TEM) images were acquired on a Philips CM-20 transmission electron microscope (Philips Technai 12) operating at a voltage of 120 kV. Scanning electron microscopy (SEM) images were obtained from an Apreo scanning electron microscopy (QUATTRO S, Thermo Scientific). The size and ζ potential were measured by a dynamic light scattering (DLS) particle-size analyzer (Malvern Zetasizer Nano ZS). Photoluminescence (PL) was obtained by an F-4600 spectrophotometer (Hitachi) with the excitation source adapted to fiber-coupled diode lasers.

Release of Pt from PPA-Pt^{IV}-NCs

PPA-Pt^{IV}-NCs (0.1 mg/mL) were dispersed in PBS (pH 7.4) containing 0.5 mM ascorbate. For the samples without irradiation, the PPA-Pt^{IV}-NCs were put into the dialysis cassettes directly to monitor the release properties at 37 °C with a shaking speed at 160 rpm (IKA[®] KS 4000 i control, protected from light). For the samples with irradiation at 808 nm, the PPA-Pt^{IV}-NCs were first irradiated by an 808 nm laser for 10 min (0.5 W/cm²) before the release experiment. The solution outside of the dialysis cassette (380 μ L) was collected at different time points (0, 1, 2, 12, 18, 24 h) and replaced by fresh PBS containing 0.5 mM ascorbate. All the collected solutions were digested by 300 μ L aqua regia at 70 °C and the Pt concentrations were determined by ICP-OES. The release of Pt after irradiation was confirmed by electrospray ionization mass spectrometry (ESI-MS).

Detection of Singlet Oxygen

The generation of singlet oxygen was detected by a 1,3-diphenylisobenzofuran (DPBF) assay. The various loaded ratios of PPA-Pt^{IV}-NCs (0.1 mg/mL NCs) were dispersed in 100 μ L DMSO containing 200 μ M DPBF. The mixtures were transferred into a 96-well plate and irradiated by an 808 nm laser (0.5 W/cm²) for different periods of time. The absorbance at 418 nm was recorded subsequently. In Figure S13, A_0 is the UV absorbance at 0 min at 418 nm, A is the UV absorbance after the indicated time points of irradiation at 418 nm.

Cell Lines and Cell Culture Conditions

4T1 and MCF-7 cells were purchased from American Type Culture Collection (ATCC) and labeled as passage 1 after reception. The two cell lines were maintained in DMEM with 10% FBS and 100 U/mL penicillin and streptomycin. A2780 and A2780cisR cells were generously provided by Prof. Wee Han Ang at the Department of Chemistry in the National University of Singapore and cultured in RPMI-1640 supported with 10% FBS, 100 IU/mL penicillin and streptomycin, and 2 mM L-glutamine. MRC-5 cells were purchased from Cell Bank of Type Culture Collection of Chinese Academy of Sciences and maintained in MEM with 10% FBS, 1% L-glutamine, 1% NEAA, and 1% sodium pyruvate. For the cisplatin-resistant cell line, 5 μ M cisplatin was added to the culture media every two passages to maintain the resistance. The MRC-5 cells used for experiments are within 10

passages after receiving the cells. All the cells were cultured in a humidified incubator at 37 °C with 5% carbon dioxide.

Time-dependent Cellular Accumulation of Pt

4T1, MCF-7, A2780, and A2780cisR cells were seeded in 6-well plates and incubated until the cell confluency reached 80%. The medium was changed to PPA-Pt^{IV}-NCs in PBS (0.1 mg/mL NCs), and incubated for another 1, 2, 4, and 6 h. After each time point of incubation, the treated cells were washed with fresh PBS for 3 times and harvested with trypsin. The cell number of each sample was recorded, and the Pt concentration of each sample was achieved from ICP-OES after aqua regia digestion overnight at 70 °C.

Determination of Photocytotoxicity in Different Cell Lines

4T1, MCF-7, A2780, A2780cisR, and MRC-5 cells were seeded in 96-well plates at a density of 3000 cells/well and further cultured for another 36 h. The cells were then treated with various concentrations (0, 0.25, 0.5, 1, and 2 µg/mL) of PPA-Pt^{IV}-NCs and ERY₁-PEG_{3k}/PPA-Pt^{IV}-NCs dissolved in PBS (pH 7.4) for 2 h. The cells were irradiated with an 808 nm laser beam for 5 min per well or kept in dark. For the small molecule, the cells were treated with 0.05, 0.1, 0.2, and 0.4 µM (Pt concentration) of PPA-Pt^{IV}-COOH, which are the same as those in 0.25, 0.5, 1, and 2 µg/mL of PPA-Pt^{IV}-NCs (22%, w/w), respectively. After incubation for 2 h, the cells were irradiated with an 808 nm (0.5 W/cm², 5 min per well) laser (for the nanoparticles) or an 660 nm laser (100 mW/cm², 5 min per well, for the small molecule), respectively. The medium containing nanoparticles in the wells were then removed, the cells in each well were washed with fresh PBS for 3 times, and further cultured for another 48 h with fresh medium. MTT assay was carried out to determine photocytotoxicity.

The equation to calculate the percentage of cell viability is below:

$$\text{Cell viability (\%)} = \frac{OD3 - OD2}{OD1 - OD2} \times 100 \%$$

where, OD1 is the average readout value of untreated cells without irradiation, OD2 is the blank (without cells), and OD3 is the readout value of the cells treated with various concentrations of nanoprodrugs or small molecule without or with irradiation. The cell viability of untreated cells without irradiation was set as 100% for calculation.

Concentration-dependent Cellular Accumulation of Pt in A2780cisR Cells

The A2780cisR cells were seeded in 6-well plates and incubated until the cell confluency reached 80%. The medium was changed to PBS (pH 7.4) containing PPA-Pt^{IV}-COOH and PPA-Pt^{IV}-NCs with various Pt concentrations for the test and incubated for 2 h. After 2 h of treatment, the supernatant was removed, the cells were washed with fresh cold PBS (pH 7.4) for 3 times, and then the cells were harvested with trypsin immediately. The cell number of each sample was counted, and the Pt concentration of each sample was detected by ICP-OES after aqua regia digestion overnight at 70 °C.

Pt Level in Genomic DNA with or without Irradiation

A2780cisR cells were seeded in 10 cm Petri dishes and incubated until the cell confluency reached 80%. The medium was changed to PBS (pH 7.4) containing PPA-Pt^{IV}-NCs at a concentration of 0.1 mg/mL NCs. After 2 h of incubation, the cells were irradiated by 808 nm (0.5 W/cm², 10 min/dish) for the irradiation group, then cells were washed with ice-cold PBS for three times; while the cells without irradiation were just washed with PBS for three times directly. After further culturing with fresh medium for 2 h, the genomic DNA of each dish was collected using a commercial kit (K0721, GeneJET Genomic DNA Purification Kit, Thermo Scientific) after washed three times with cold PBS and trypsinization. The DNA concentration was quantitated by UV-Vis spectroscopy (NanoDrop One Microvolume UV-Vis Spectrophotometer, Thermo Scientific). The amount of platinum in the genomic DNA was determined by ICP-MS. The concentration of platinum was expressed as ng of platinum mg DNA.

Intracellular ROS Detection

The intracellular ROS detection was determined by 2',7'-dichlorodihydrofluorescein diacetate (H₂DCFDA). A2780cisR cells were seeded in 35 mm glass-bottom confocal dishes with a density of 3×10^5 cells per dish. After 36 h, the cells were treated with PPA-Pt^{IV}-NCs dissolved in PBS (pH 7.4) at a concentration of 0.1 mg/mL NC for 2 h. After 2 h incubation, one group treated with PPA-Pt^{IV}-NCs was irradiated by 808 nm (0.5 W/cm², 10 min) as the irradiation group, then cells were washed with ice-cold PBS for three times and stained by 10 μM H₂DCFDA for 30 min. For the other group, cells treated with PBS alone were used as negative control. The cells treated with 3 mM H₂O₂ in PBS for 15 min were set as the positive control. The PPA-Pt^{IV}-NCs group without irradiation was used as a comparison. H₂DCFDA was further added in these three groups and the cells were incubated for another 30 min in 37 °C, protected from light. The confocal images were obtained with a confocal microscope (Leica SP5) excited at 405 nm and detected from 650 nm to 700 nm.

PEGylation of PPA-Pt^{IV}-NCs

O-[N-(6-maleimidohexanoyl)aminoethyl]-O'-[3-(N-succinimidylxy)-3-oxopropyl]polyethylene glycol 3,000 (NHS-PEG_{3k}-MAL) was covalently conjugated with the nanoplatfrom through the free NH₂ groups remained on PPA-Pt^{IV}-NCs. NHS-PEG_{3k}-MAL (1 mg) was dissolved in 50 mL phosphate buffered saline (PBS, pH 8.0), and the concentration was 0.02 mg/mL. The sample was stirred overnight to modify the free NH₂ groups on PPA-Pt^{IV}-NCs with NHS-PEG_{3k}-MAL solution at the ratio of 50:1 (w/w) in PBS (pH 8.0) in the dark at room temperature. The extra NHS-PEG_{3k}-MAL was removed by dialysis (SnakeSkin Dialysis Tubing, 10 K MWCO) against water for 48 h (protected from light). The synthesized PEGylated PPA-Pt^{IV}-NCs (PEG_{3k}/PPA-Pt^{IV}-NCs) were stored at 4 °C (in the dark) for further investigations and modifications.

Synthesis of ERY₁-PEG_{3k}/PPA-Pt^{IV}-NCs

ERY₁ peptide was covalently conjugated with PEG_{3k}/PPA-Pt^{IV}-NCs through the reaction of thiol-reactive maleimide group on the distal end of 3 kDa PEG and the C-terminus cysteine residue of the ERY₁ peptide. The ERY₁ peptide was dissolved in a 1:1 mixture of DMSO and PBS at a concentration of 0.1 mg/mL, and added to

the PEG_{3k}/PPA-Pt^{IV}-NCs dropwise with a ratio of 1:50 (w/w) under gently stirring overnight. The reactions were protected from light and stirred overnight at room temperature. After that, the liquid in reactions was used for quantification of peptide conjugation rate immediately, and the rest was purified by dialysis (SnakeSkin Dialysis Tubing, 10 K MWCO) against water for 48 h (protected from light). The synthesized ERY₁-PEG_{3k}/PPA-Pt^{IV}-NCs were subsequently resuspended in PBS (pH 7.4) at 4 °C (in the dark) for further investigations and modifications.

Stability of PPA-Pt^{IV}-COOH, PPA-Pt^{IV}-NCs, and ERY₁-PEG_{3k}/PPA-Pt^{IV}-NCs in Fresh Mouse

Whole Blood

The stability of Pt^{IV} in fresh mice whole blood was tested by high-performance liquid chromatography (HPLC). Firstly, PPA-Pt^{IV}-COOH (250 μM) was dissolved in 0.7 mL fresh mice whole blood (containing 0.5% DMF). The mixture was incubated at 37 °C for certain hours. At each time point, a 100 μL whole blood mixture was transferred to a new tube containing 300 μL of methanol to precipitate proteins in the blood. The tube was vortexed for 1 min at room temperature, and then centrifuged at 14,000 g, 4 °C for 5 min to collect the supernatant. Subsequently, the supernatant was filtered with a 0.22 μm filter before HPLC examination. The HPLC chromatogram was recorded at 420 nm, at this wavelength PPA and PPA-Pt^{IV}-COOH share the same molar extinction coefficient; therefore, the amount of detected PPA can be used to represent the amount of reduced PPA-Pt^{IV}-COOH. Solvent A (H₂O with 5% acetonitrile and 0.1% TFA) and solvent B (acetonitrile with 5% H₂O and 0.1% TFA) were used for a gradient elution at a flow rate of 1.0 mL/min. The samples were eluted by using a program as follows: 0% B (0 min) → 20% B (7 min) → 100% B (12 min) → 100% B (25 min) → 0% B (27 min) → 0% B (30 min). The remained PPA-Pt^{IV}-COOH (%) at each time point is calculated based on the following equation: remained Pt^{IV} % = $A_{Pt}/(A_{Pt}+A_{PPA})$, where A_{Pt} and A_{PPA} are the area of PPA-Pt^{IV}-COOH and PPA detected in the supernatant of test samples, respectively.

For the stability of Pt^{IV} in PPA-Pt^{IV}-NCs and ERY₁-PEG_{3k}/PPA-Pt^{IV}-NCs, PPA-Pt^{IV}-NCs and ERY₁-PEG_{3k}/PPA-Pt^{IV}-NCs were added into 0.7 mL fresh mice whole blood, resulting in a final concentration of 250 μM Pt. Then the nanoparticles were incubated in the blood at 37 °C for certain hours. At each time point, a 100 μL mixture was immediately transferred to a new tube containing 300 μL of methanol to precipitate the proteins and nanoparticles in the blood. The tube was vortexed for 1 min at room temperature, and centrifuged at 14,000 g, 4 °C for 5 min. The supernatant that contains the released PPA was collected and filtered with a 0.22 μm filter for HPLC examination. The total concentration of Pt^{IV} prodrug in the nanoparticles system is 250 μM, which means if all the Pt^{IV} are decomposed, a total of 250 μM PPA could be released from the nanoparticles. Therefore, as a standard control, 250 μM of PPA was added into the mixture of 100 μL fresh mice whole blood, followed by ethanol precipitation, as described above. The supernatant was collected and examined by HPLC as the standard control, which represented the maximum amount of PPA that could be released from the nanoparticles. The remained Pt^{IV} in PPA-Pt^{IV}-NCs and ERY₁-PEG_{3k}/PPA-Pt^{IV}-NCs is calculated based on the following equation: remained Pt^{IV} % = $(A_{PPA'}-A_{PPA''})/A_{PPA'}$, where $A_{PPA'}$ is the area of the 250 μM PPA standard; $A_{PPA''}$ is the area of PPA (from decomposed Pt^{IV}) detected in the supernatant of the test samples at different time points, respectively.

The HPLC chromatogram was recorded at 420 nm as mentioned above. The half-lives were calculated by GraphPad Prism software.

Blood Collection and Preparation of Erythrocytes Binding *In Vitro*

Fresh mouse whole blood was collected through retro-orbital sinus/plexus puncture from deep anesthesia mice.⁶ The tubes for blood collection were pre-sprayed by 20 μ L heparin sodium (TCI) (25 IU/mL) solution.⁷ After collection, the tubes were inverted 3-6 times to completely mix the blood with the anticoagulant, and stored in the dark at 4 °C for further usage. For the collection of erythrocytes, the fresh whole blood was first pipetted out and centrifuged at 800 \times g for 10 min (4 °C) to separate the buffy coat and plasma.⁸ Then the collected erythrocytes pellet were washed three times with cold PBS (pH 7.4) by centrifugation at 800 \times g for 10 min (4 °C), and subsequently resuspended in PBS and kept on ice or stored in 4 °C for further use.

The binding processes of erythrocytes with ERY₁-modified PEG_{3k}/PPA-Pt^{IV}-NCs or PEG_{3k}/PPA-Pt^{IV}-NCs were described as below. 100 μ L of the prepared erythrocytes solution (1×10^9 cells/mL) was pipetted, and the cells were resuspended in 1 mL albumin bovine (BSA) (Fraction V, for biochemistry, pH 7.0, ACROS Organics™) solution (5 mg/mL, in PBS, pH 7.4) in a sterile tube. The erythrocytes in the tube were further incubated overnight at 4 °C in the dark with gentle vortex continuously to avoid nonspecific binding. The ERY₁-PEG_{3k}/PPA-Pt^{IV}-NCs or PEG_{3k}/PPA-Pt^{IV}-NCs (0.1 mg/mL NCs, 50 μ L) were consequently added to the BSA-precoated erythrocytes and further vortexed for another 12 h. The binding processes were stopped by washing twice with PBS at 800 \times g for 10 min (4 °C) through centrifugation, and the pellets were resuspended in cold PBS (pH 7.4) for further analysis. The binding processes of BSA-precoated erythrocytes with other complexes were prepared in the same way mentioned above. All the processes were protected from light.

Confocal Imaging Assessment for Erythrocytes Binding

All the erythrocyte samples after binding processes were firstly monitored by confocal microscopy. The as-prepared erythrocytes of different groups were seeded at 1×10^7 cells/dish into the 3.5 mm diameter glass-bottom confocal dishes (NEST) in PBS (pH 7.4). All imaging was acquired through a confocal microscope (Leica SP5) with constant acquisition and display parameters. The excitation wavelength was 405 nm, and the detected range for emission was 650 – 700 nm. The fluorescence intensity of different groups was further quantified as the corrected total cryosection fluorescence (CTCF) by ImageJ software (NIH) for each confocal image. One hundred and fifty erythrocytes from each group were counted for quantification.

Sample Preparation for Scanning Electron Microscope (SEM)

The samples (erythrocytes only and erythrocytes incubated with PEG_{3k}/PPA-Pt^{IV}-NCs or ERY₁-PEG_{3k}/PPA-Pt^{IV}-NCs) were first fixed with primary fixative (2.5% glutaraldehyde and 2% paraformaldehyde in 0.1 M cacodylate buffer (pH 7.2) with 0.05% CaCl₂) on Thermanox tissue culture coverslips (with cells face up, pre-coated with poly-L-lysine) for 2 h at room temperature (RT). Then the coverslips with sample were rinsed three times with PBS for 5 min at RT and washed twice with PBS for 10 min at RT, respectively. Samples further got secondary fixation with 2% OsO₄ in 0.1 M cacodylate buffer (pH 7.2) for another 2 h at RT. After that, samples were rinsed another

three times with PBS for 5 min at RT as before, then the samples were further washed twice with PBS for 10 min at RT, and ddH₂O twice, 10 min per time, for the dehydration process. In the dehydration part, the samples were dehydrated with 30% ethanol (5 min, RT), 50% ethanol (5 min, RT), 70% ethanol (5 min, RT), 80% ethanol (5 min, RT), 90% ethanol (5 min, RT), 95% ethanol (5 min, RT), 100% ethanol (10 min, RT), 100% ethanol (10 min, RT), 100% ethanol:100% acetone (3:1) (10 min, RT), 100% ethanol:100% acetone (1:1) (10 min, RT), 100% ethanol:100% acetone (1:3) (10 min, RT), 100% acetone (15 min, RT), 100% acetone (15 min, RT), 100% acetone (15 min, RT). Then the samples were followed with Critical Point Drying (CPD) in liquid CO₂ (BAL-TEC CPD 030), and the samples in acetone (the sample slips soaked in acetone before the machine work) in the machine were gradually replaced by the liquid CO₂, and kept in CO₂ Critical Point Drying at 10 °C, 60 min. At last, the samples were ready for the SEM.

Flow Cytometry for Erythrocyte Binding Assessment

The fluorescence signals of erythrocytes in the three groups mentioned above were measured by a CytoFLEX S flow cytometry (Beckman Coulter, USA). All the samples were tested with the excitation wavelength of 638 nm and a detection wavelength at 660 nm (APC channel) for the signal of PPA on erythrocytes. The signal from 10,000 events was collected for each sample. Based on the flow cytometric data, the fluorescence signal of each sample was analyzed by FlowJo software. The percentage of cells positive for binding was computed from the histogram plot calculated from triplicate measurements of each sample.

Flow Cytometry for Erythrocyte Binding Assessment with GYPA Antibody

The binding rate of the complexes on erythrocyte was further determined by flow cytometry after incubated with glycophorin A (GYPA) antibody. The test processes were listed below. The erythrocytes after the binding processes with various complexes described above were further incubated with anti-mouse glycophorin A polyclonal antibody (ALEXA FLUOR® 488 conjugated, bs-2575R-A488, Bioss Antibodies) overnight at 4 °C, protected from light. The measurement can be applied to further confirm that the nanoprodruag was bound on the erythrocytes through the GYPA docking. All the samples for the flow cytometry were tested with the excitation wavelength of 488 nm and a detection wavelength at 530 nm (Alexa 488 channel) for the signal of GYPA antibody on erythrocytes. Appropriate gating was established by using the antibody as the positive control, while the group of erythrocytes only was applied as a negative control.

ICP-OES to Detect Conjugated Pt on Erythrocyte

The Pt content of all the erythrocyte samples after binding processes above was further determined by ICP-OES. The cell number of erythrocytes (erythrocytes with modified ERY₁-PEG_{3k}/PPA-Pt^{IV}-NCs, or PEG_{3k}/PPA-Pt^{IV}-NCs) after binding to complexes were counted in each sample, the erythrocytes were further harvested by centrifugation, and the Pt concentration of each sample was detected by ICP-OES after aqua regia digestion overnight at 70 °C.

Maximum Tolerated Dose of ERY₁-PEG_{3k}/PPA-Pt^{IV}-NCs *In Vivo*

After determination of the binding capacity of the ERY₁-PEG_{3k}/PPA-Pt^{IV}-NCs to erythrocytes *in vitro*, the maximum tolerated dose (MTD) of ERY₁-PEG_{3k}/PPA-Pt^{IV}-NCs was determined in nine BALB/c mice with 6 to 8 weeks of age before other *in vivo* evaluations. The MTD was determined by observing the progression of the mice treated at various doses of complexes using the same procedures described below. ERY₁-PEG_{3k}/PPA-Pt^{IV}-NCs were dissolved and prepared in 0.9 % NaCl with different doses (based on Pt content) at 1.5, 2.5, 3.5 $\mu\text{mol-Pt/kg}$, and intravenously injected once for each mouse ($n = 3$). Body weights, changes in behavior, and sign of distress were recorded. The dose at which neither debilitating effects nor sign of distress was observed and set as the MTD. The MTD dose was confirmed by treating a cohort of at least 3 mice per complex and monitored every day for 14 days.

Pharmacokinetic Test *In Vivo*

Pharmacokinetic test in blood *in vivo* was determined in nine healthy BALB/c mice with 6-7 weeks old and 15-18 g of body weight. All the nine mice were divided into 3 groups ($n = 3$) randomly: a) group of PPA-Pt^{IV}-COOH, b) group of PEG_{3k}/PPA-Pt^{IV}-NCs, and c) group of ERY₁-PEG_{3k}/PPA-Pt^{IV}-NCs. The samples were intravenously injected (single dose) into each mouse as indicated through tail vein. The injection dose was 1.3 $\mu\text{mol-Pt/kg}$ for each group, and the injection volume was based on 0.4 mL/20 g body weight. For the group of PPA-Pt^{IV}-COOH, the injection solvent containing 0.6% DMF from PPA-Pt^{IV}-COOH stock solution in 0.9% NaCl, and concentration of 1.3 $\mu\text{mol-Pt/kg}$ is determined by the solubility property of PPA-Pt^{IV}-COOH in the solvent. For the groups of PEG_{3k}/PPA-Pt^{IV}-NCs and ERY₁-PEG_{3k}/PPA-Pt^{IV}-NCs, only 0.9% NaCl worked as the vehicle, and the concentration was 1.3 $\mu\text{mol-Pt/kg}$ as well. The whole blood was collected by retro-orbital puncture from each anesthetized mouse at ten continuous time points (30 - 80 $\mu\text{L/time point}$). The time points were 6 min, 1 h, 4 h, 25h (1 d), 53.3 (2 d), 77 h (3 d), 115.5 h (5 d), 193.5 h (8 d), 289 h (12 d), and 336 h (14 d). Then the volume of whole blood at each time point was first carefully quantified, pipetted, and digested with aqua regia overnight at 70 °C for ICP-OES test. The pharmacokinetics parameters were analyzed by PKsolver software.⁹ For PPA-Pt^{IV}-COOH and ERY₁-PEG_{3k}/PPA-Pt^{IV}-NCs, the curves fit the first-order kinetics elimination for the One-Compartment Open Model: Intravenous Bolus Administration for analysis. For PEG_{3k}/PPA-Pt^{IV}-NCs, the curve fits the Two-Compartment Open Model: Intravenous Bolus Administration for analysis.

Bioimaging and Biodistribution *In Vivo*

With the photo-controllable Pt(IV) prodrug on the nanoparticles, the maximum accumulation time point of complexes can be determined for *in vivo* anticancer evaluation in the animal with a tumor. Besides, the function of erythrocytes as a carrier was further confirmed by this *in vivo* experiment. Thus, the *in vivo* fluorescence bioimaging was applied in mice bearing 4T1 xenograft tumor.

The 4T1 xenograft tumor model was established on twenty BALB/c mice by subcutaneously (*s.c.*) injection of 4T1 murine breast cancer cells (1×10^6 cell/0.1 mL/mouse). The cancer cells were implanted in the right axillary fossa of BALB/c mice with 6-week-old, 16 - 18 g body weight. Tumor nodules were allowed to grow 9 days to

achieve a volume of 500 - 800 mm³ before the injection of the complexes. The twenty mice were divided into 5 groups as: i) control group; ii) PPA-Pt^{IV}-COOH group; iii) PPA-Pt^{IV}-NCs group; iv) PEG_{3k}/PPA-Pt^{IV}-NCs group; and v) ERY₁-PEG_{3k}/PPA-Pt^{IV}-NCs group. Four mice in each group were intravenously injected with 1.3 μmol-Pt/kg of various complexes as indicated above. The dose was lower than the MTD, and it's the highest dissolution of PPA-Pt^{IV}-COOH with 0.63% of DMF in 0.9% NaCl. Other complexes were dissolved in 0.9% NaCl directly. Besides, 0.9% NaCl was used in the untreated group. The mice were anesthetized with 50 mg/kg phenobarbital via intraperitoneal (*i.p.*) injection before imaging. The hair on the tumor and abdomen was removed by hair clipper and depilatory cream. The *in vivo* imaging was acquired at each time point (5 min, 3 h, 17 h, and 24 h) by Bruker In Vivo-Xtreme with excitation at 650 nm and emission at 670-750 nm. One mouse from each group was further sacrificed to collect heart, liver, spleen, lung, kidneys, and tumor immediately. The fluorescence bioimaging was applied for these organs using the same machine and parameter. After images were acquired, the organs were subsequently digested with aqua regia overnight at 90 °C for ICP-OES test after weighed, homogenated, and lyophilized. Images were processed with Bruker MI SE software to quantify the fluorescence intensity in the tumor. The experiment was finished as two independent tests.

Anticancer Evaluation in 4T1 Xenograft Model

4T1 tumor-bearing xenograft model was established in BALB/c mice via the same inoculation procedures mentioned above. After 7 days, the tumor nodules reached around 100 mm³ before the initiation of treatment. All the mice were numbered with ear tags, and the mice with tumor within the range were divided into eight groups randomly (n = 5): i) 0.9% saline; ii) 0.9% saline with 7 times of 808 nm irradiation (Day 0 - 6); iii) PPA-Pt^{IV}-COOH at 2.5 μmol-Pt/kg (containing 0.2% DMF and 4.5% Kolliphor HS 15 in 0.9% saline); iv) PPA-Pt^{IV}-COOH at 2.5 μmol-Pt/kg (containing 0.2% DMF and 4.5% Kolliphor HS 15 in 0.9% saline) with 660 nm irradiation once (Day 0); v) PEG_{3k}/PPA-Pt^{IV}-NCs at 2.5 μmol-Pt/kg in 0.9% saline with 7 times of 808 nm irradiation (Day 0 - 6); vi) ERY₁-PEG_{3k}/PPA-Pt^{IV}-NCs at 2.5 μmol-Pt/kg in 0.9% saline without 808 nm irradiation; vii) ERY₁-PEG_{3k}/PPA-Pt^{IV}-NCs at 2.5 μmol-Pt/kg in 0.9% saline with 3 times of 808 nm irradiation (Day 0 - 2); and viii) ERY₁-PEG_{3k}/PPA-Pt^{IV}-NCs at 2.5 μmol-Pt/kg in 0.9% saline with 7 times of 808 nm irradiation (Day 0 - 6). All the mice were applied with intravenous (*i.v.*) injection only once on Day 0. Three hours after injection, mice were anesthetized with phenobarbital and the hair shaved tumors were irradiated with a 660 nm laser for 10 min per mouse at a light dose of 100 mW/cm², or 808 nm laser for 30 min (5 min irradiation with 5 min interval) per mouse at the power density of 0.5 W/cm². For 660 nm irradiation, the tumors were exposed to the 660 nm laser once three hours after the *i.v.* injection on Day 0. For 3 times of 808 nm irradiation, the tumors were exposed to the 808 nm laser three hours after the *i.v.* injection on Day 0 (1st time of irradiation), and the 2nd, 3rd times of irradiation were applied on Day 1 and Day 2. While for 7 times of 808 nm irradiation, the laser was applied in the same approach, and the frequency was increased to 7 times (one irradiation per day till Day 6). The tumor size and body weight were monitored every two days for a total of 14 days. All the mice were sacrificed when the tumor size of the control group exceeded 2000 mm³. The excised tumors and vital organs (heart, liver, spleen, lung, kidneys) were weighed and collected once the experiment was terminated. Tumor length and width were measured with calipers, and the tumor volume was calculated using the following equation: $TV=(a)(b^2)\pi/6$, where a is the

longest dimension and b is the largest dimension orthogonal to a. Statistical analysis was performed using Student's t-Test at the endpoint. The blood of each mouse was collected for the biochemistry test. The experiment was finished as two independent tests.

T Cell Measurement in Tumor by Flow Cytometry

When the anticancer evaluation finished on Day 14, the mice of each group were sacrificed immediately after blood collection. The mice body were soaked in 75% alcohol, and tumors were surgically removed and collected on ice. The dissociation of cells from primary tissues (tumors) was prepared by trypsin.^{10, 11} After dissecting off unusable tissue, the remaining tissue was minced into 3 - 4 mm pieces with a sterile scalpel or scissors. The tissue pieces were washed by resuspending in a balanced salt solution without calcium and magnesium. After the tissue pieces were settled, the supernatant was removed. The washing step was repeated for 3 times. Then the tubes with the tissue pieces were placed on ice, and the remaining supernatant was removed. 0.25% trypsin (Gibco®) was added with a ratio of 1 mL of trypsin for every 100 mg of tissue. The samples in the tubes were incubated at 4 °C overnight to maximize the penetration of the enzyme with minimum trypsin activity. The trypsin from the tissue pieces was further discarded by centrifugation at 500 g for 10 min at 4 °C. The samples were subsequently washed by cold PBS twice through centrifugation. All the supernatant was removed and replaced by 2 mL erythrocyte lysis buffer (eBioscience) to lyse erythrocytes for 4 - 5 min at RT. The lysis was further stopped by adding 12 mL PBS after incubation. After that, the as-prepared mouse splenocyte and tumor single-cell suspension were filtered through 70 µm cell strainers supported by 50 mL of polypropylene pipe. Then the cells were washed twice in PBS by centrifugation at 500 g for 10 min. The isolated mouse tumor single-cell were consequently stained with combinational fluorochrome-conjugated anti-mouse antibodies: anti-mouse CD3, anti-mouse CD4, and anti-mouse CD8a (eBioscience) as the immune cell surface markers and analyzed by flow cytometry. Three tumors from each group were chosen randomly for the detection. The signal from 40,000 events was collected for each sample.

Histology

The tissues (heart, liver, spleen, lung, kidneys, and tumor) were collected after experiment termination, fixed with 10% paraformaldehyde at room temperature for 48 hours, then washed with PBS once for 10 min, and Milli-Q twice for 10 min each. The samples were dehydrated with different concentrations of ethanol increased from 30% to 100% for 20 min each time. After that, the tissues were embedded in paraffin after cleared with xylene and cut into 5-µm-thick slides for hematoxylin and eosin (H&E) staining. The samples were subsequently mounted under a glass coverslip with Permount mounting medium (Fisher Chemical) and observed under a microscope with a digital camera (Nikon Eclipse 90i).

Blood Biochemistry Measurement

The hematological analysis was applied to examine the effects of the treatment for a safety evaluation after termination of the anticancer evaluation. According to the related publications,¹²⁻¹⁴ some related biochemical parameters in blood were selected for the hematological analysis, such as aspartate transaminase/serum

glutamic-oxaloacetic transaminase (AST/SGOT), alanine aminotransferase/serum glutamic-pyruvic transaminase (ALT/SGPT), creatinine, blood urea nitrogen (BUN), and uric acid (UA). On Day 14 of the anticancer evaluation in the 4T1 xenograft model, the blood was collected from each mouse for the tests. The blood plasma was subsequently collected as the supernatant after centrifugation at 800 g for 10 min at 4 °C, and the blood biochemical parameters were determined by commercial kits.

Animal Ethics

All BALB/c mice were bought from the Chinese University of Hong Kong and the City University of Hong Kong, maintained under pathogen-free conditions at the City University of Hong Kong. All animal procedures were performed following the Guidelines for Care and Use of Laboratory Animals of the City University of Hong Kong and approved by the Animal Ethics Committee of the City University of Hong Kong.

Statistics Analysis

All the results were expressed as Mean \pm SD where applicable. GraphPad Prism 8 (GraphPad Software) and Microsoft Excel were used for statistical analysis.

Results

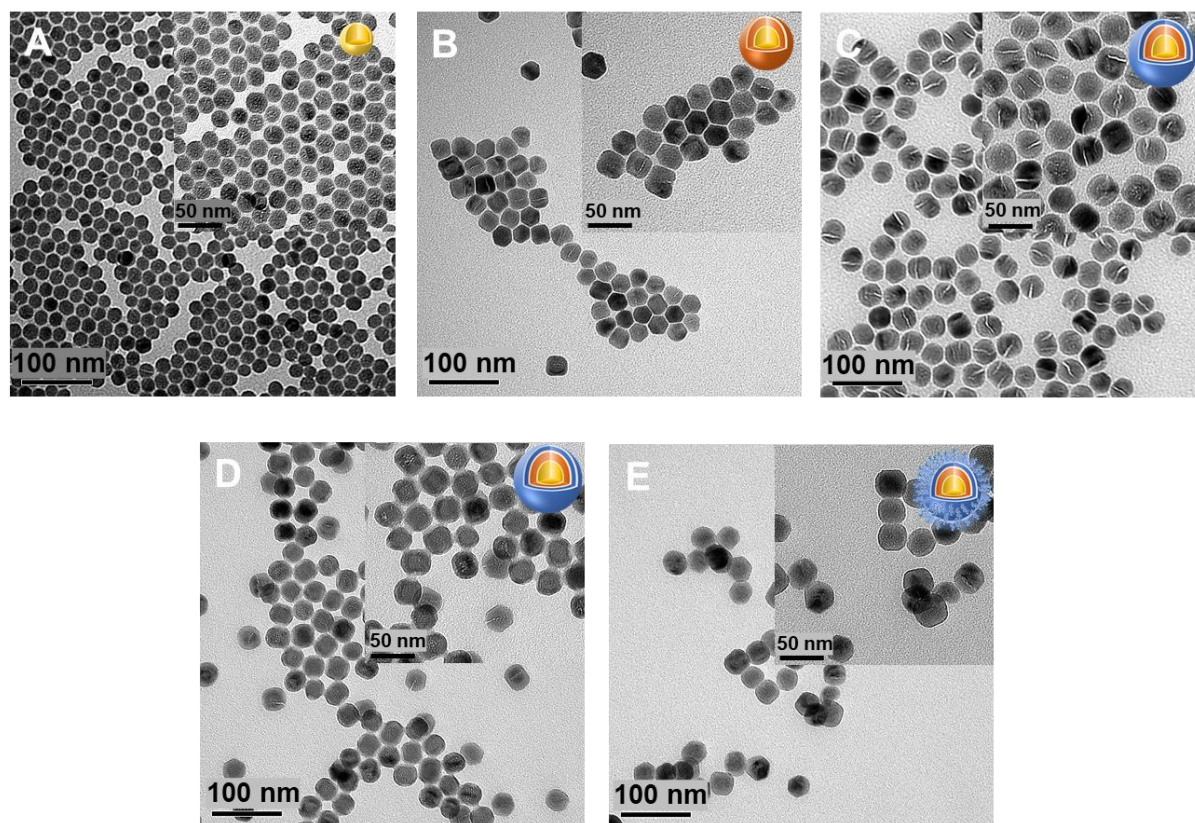


Fig. S1 TEM images of **A)** core, **B)** core-shell, **C)** core-shell-shell NCs with OA ligand (OA-NCs), **D)** ligand-free core-shell-shell NCs, and **E)** core-shell-shell NCs covered with PEI (PEI-NCs). Scale bars are 100 nm for the images and 50 nm for inserted images.

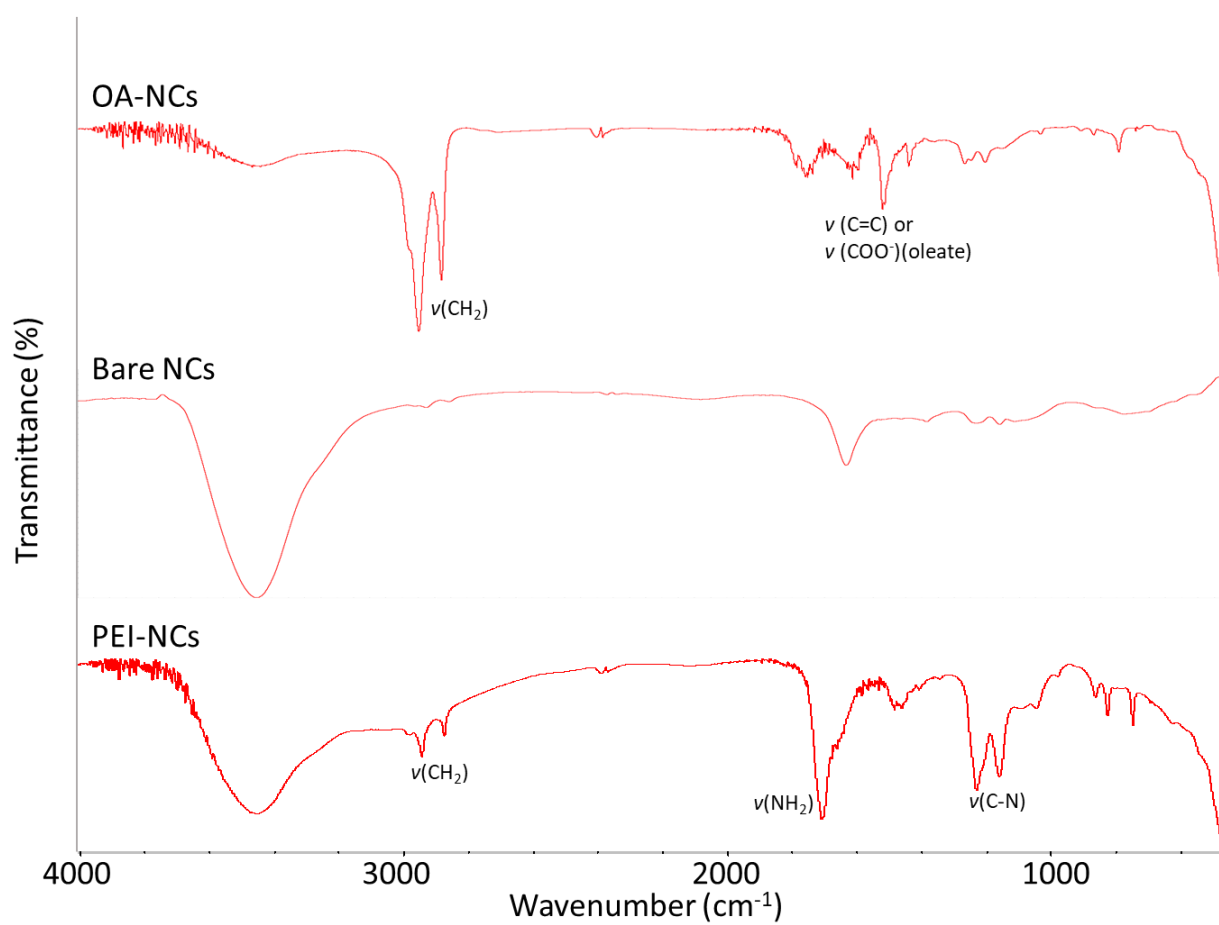


Fig. S2 FT-IR spectra of OA-NCs, bare NCs, and PEI-NCs.

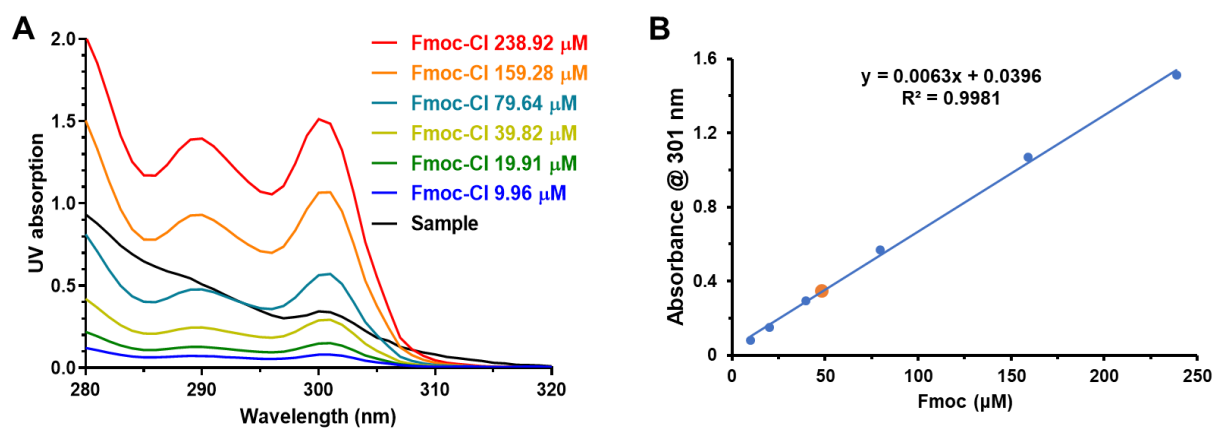


Fig. S3 UV absorbance spectra of **A)** sample solution and standard solutions containing different concentrations of Fmoc and **B)** standard curve of various concentrations of Fmoc and the sample solution at $\lambda = 301$ nm.

The presence of free amine moieties of PEI-NCs is essential for subsequent modification. The content of amine moieties on NCs was determined via a standard Fmoc quantification protocol and quantified as 0.242 mmol/g. The conjugation rate of Pt(IV) prodrug on NCs was calculated as high as 85.4%.

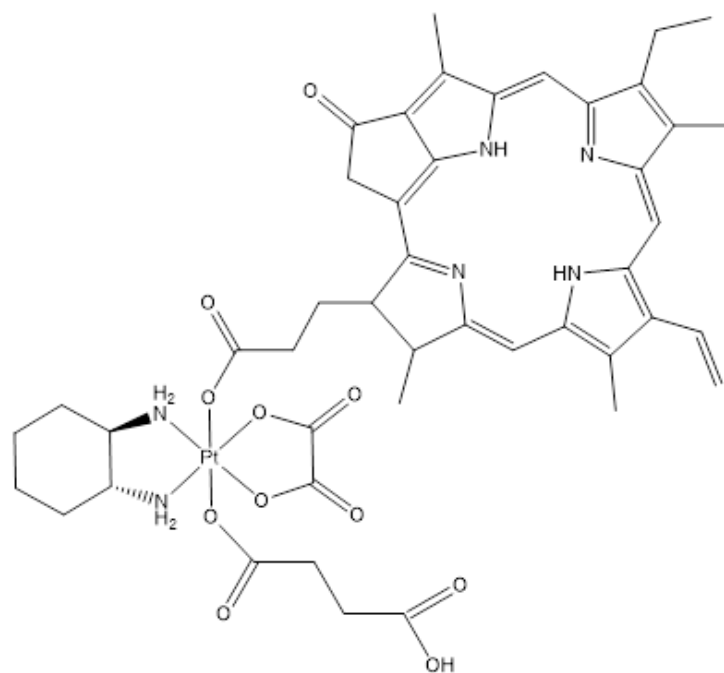


Fig. S4 Chemical structure of PPA-Pt^{IV}-COOH.

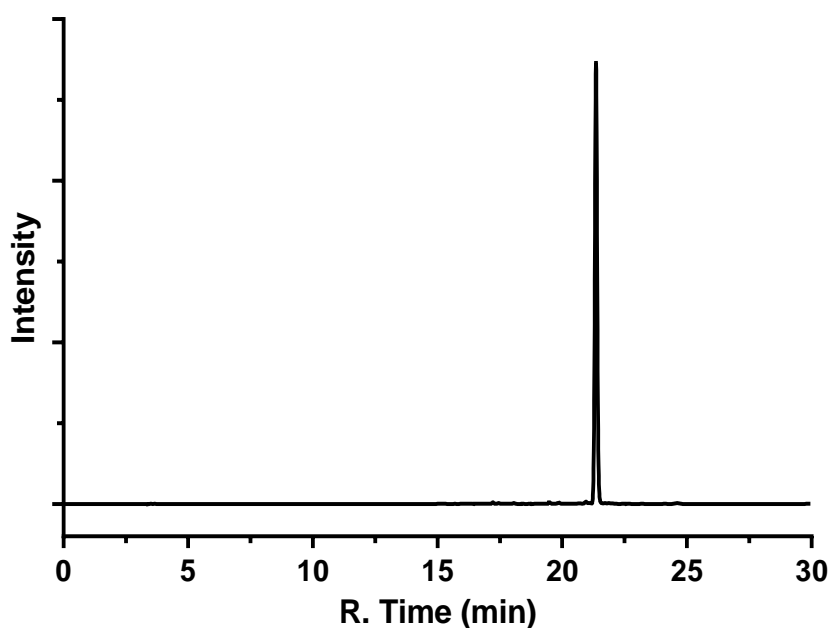


Fig. S5 RP-HPLC (420 nm) chromatograms of PPA-Pt^{IV}-COOH. Analytical reversed-phase High-Performance Liquid Chromatography (RP-HPLC) was conducted on a Shimadzu Prominence LC-20AT HPLC system equipped with a reversed-phase C18 column (Phenomenex Garmin 250 × 4.60 mm, 5 μm, 110 Å). Test samples were monitored by UV absorbance at 420 nm: Solvent A (H₂O with 5% acetonitrile and 0.1% TFA) and solvent B (acetonitrile with 5% H₂O and 0.1% TFA) were used for a gradient elution at a flow rate of 1.0 mL/min. The test samples were eluted by using a program as follows: 0% B (0 min) → 20% B (7 min) → 100% B (12 min) → 100% B (25 min) → 0% B (27 min) → 0% B (30 min).

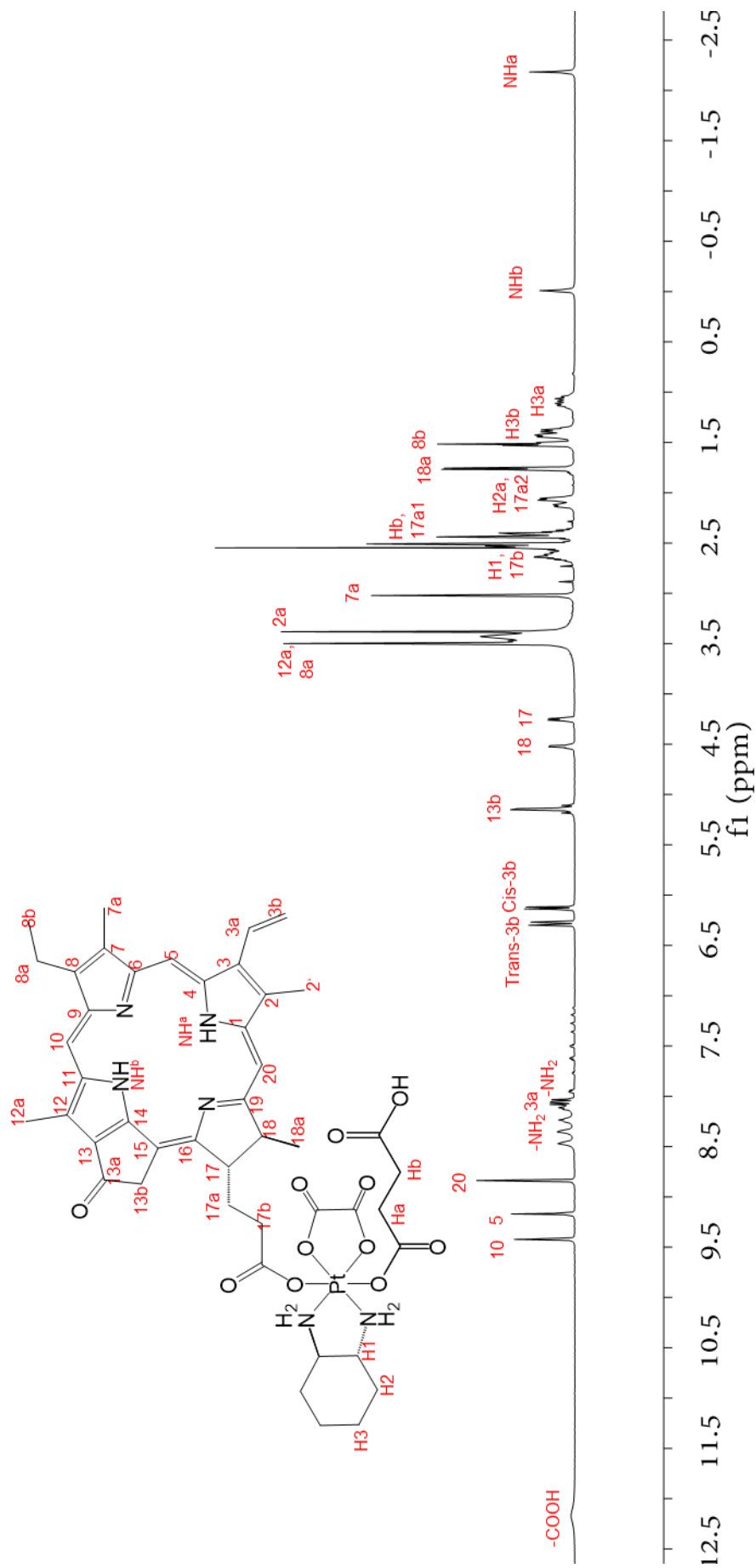


Fig. S6 ¹H NMR of PPA-Pt^{IV}-COOH.

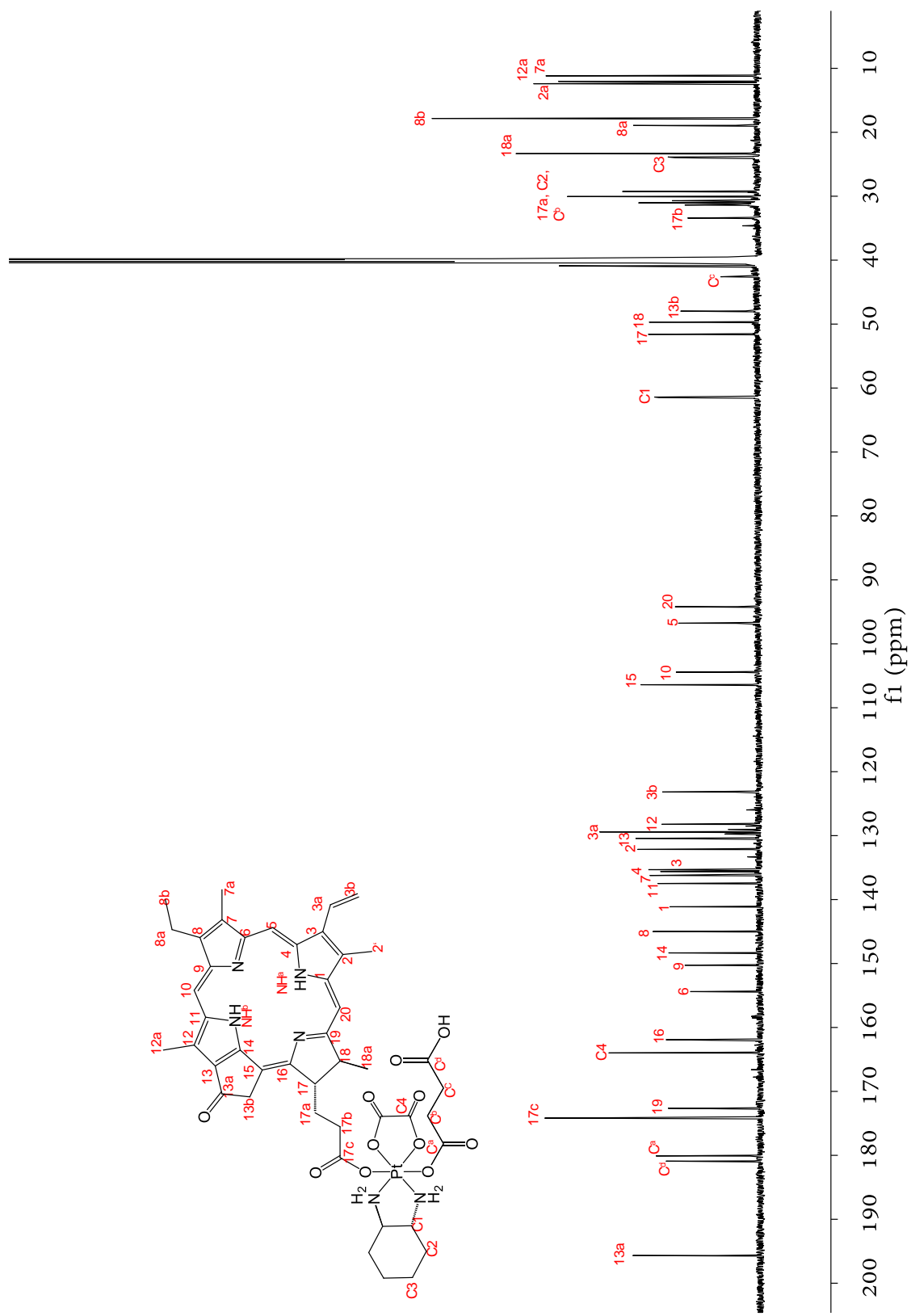


Fig. S7 ¹³C NMR of PPA-Pt^{IV}-COOH.

96.0191

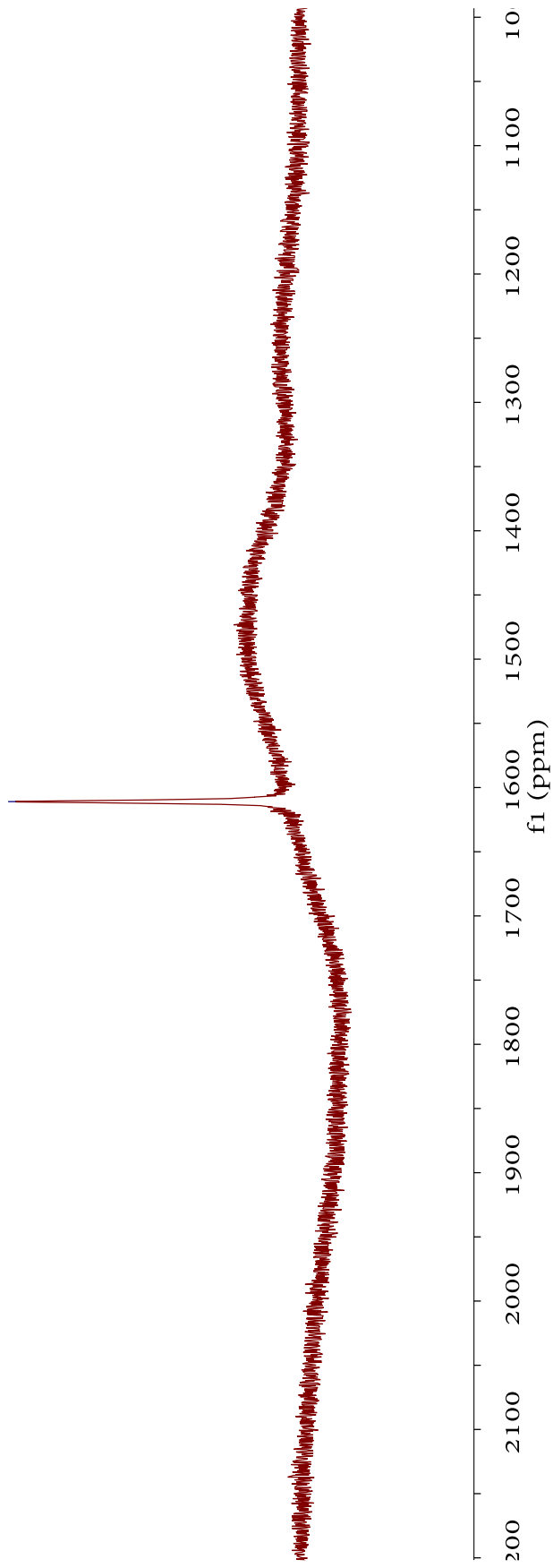


Fig. S8 ^{195}Pt NMR of PPA- Pt^{IV} -COOH.

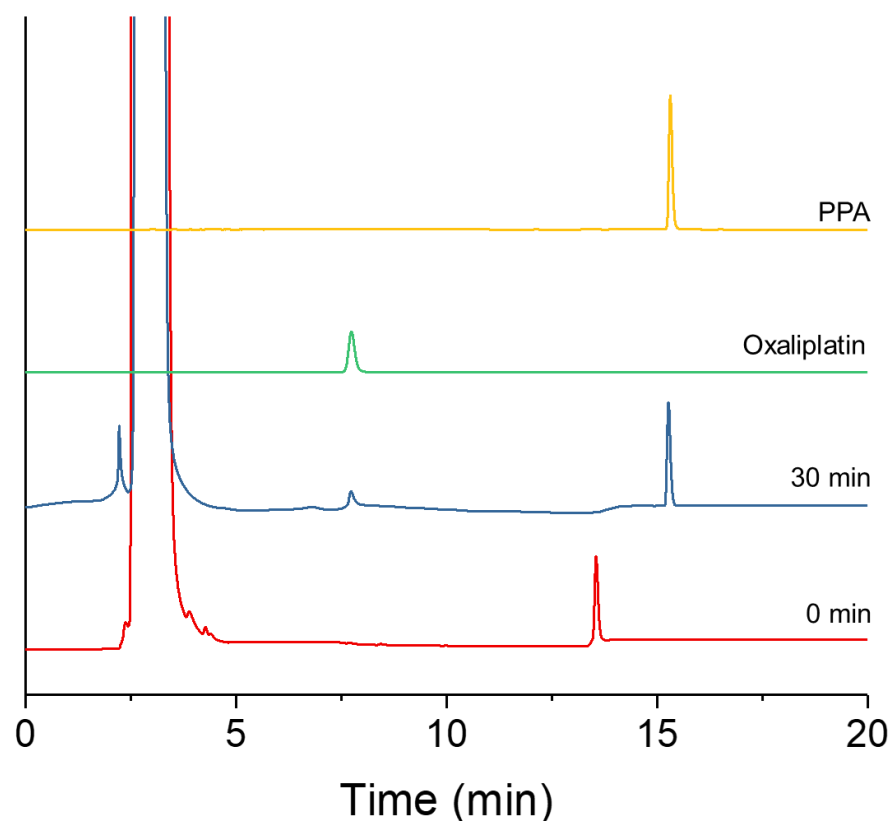


Fig. S9 The photoactivation property of PPA-Pt^{IV}-COOH tested through HPLC at 220 nm. PPA-Pt^{IV}-COOH (10 μ M) was dissolved in PBS buffer containing 1 mM sodium ascorbate. The solution was irradiated with red light (660 nm, 7 mW/cm²) for 30 min. Eluent condition: 0 min – 8 min 100% water + 0% acetonitrile – 70% water + 30 % acetonitrile; 8 min – 12 min 70% water + 30 % acetonitrile – 10% water + 90% acetonitrile; 12-20 min 10% water + 90% acetonitrile.

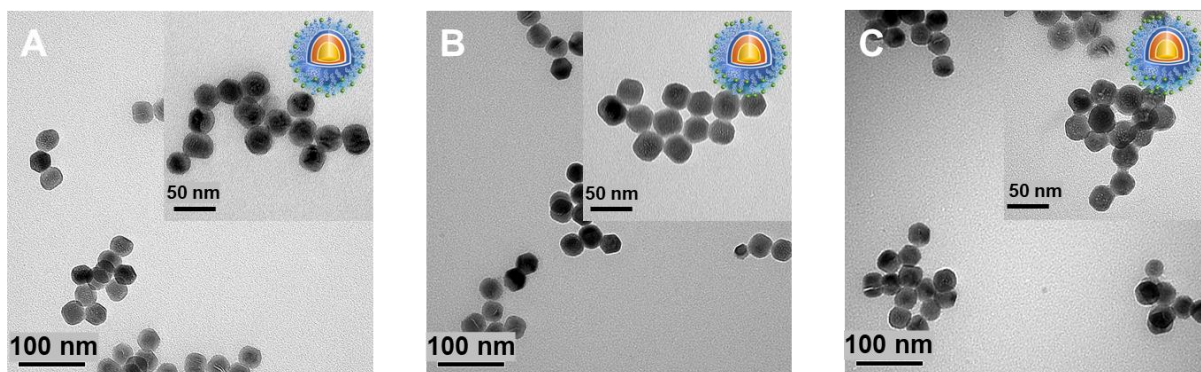


Fig. S10 TEM images of **A)** PPA-Pt^{IV}-NCs (4%, w/w), **B)** PPA-Pt^{IV}-NCs (18%, w/w), and **C)** PPA-Pt^{IV}-NCs (22%, w/w). The ratios of loaded Pt(IV) to NCs are indicated in the parentheses. Scale bars are 100 nm for the images and 50 nm for inserted images.

The TEM images show the typical morphology of NCs for PPA-Pt^{IV}-NCs with different amounts of loaded Pt(IV) prodrug.

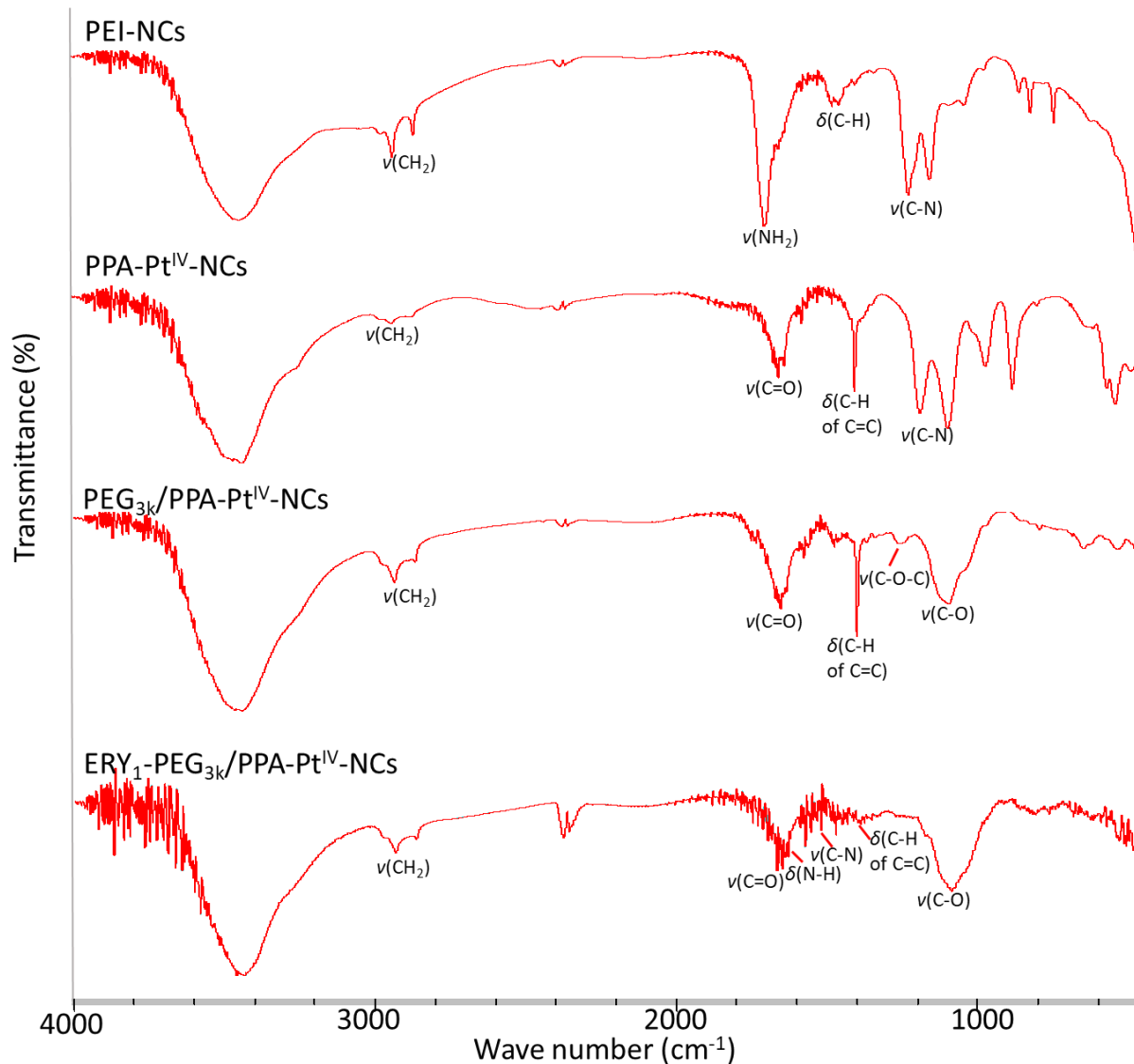


Fig. S11 FT-IR spectra of PEI-NCs, PPA-Pt^{IV}-NCs, PPA-Pt^{IV}-NCs, PEG_{3k}/PPA-Pt^{IV}-NCs, and ERY₁-PEG_{3k}/PPA-Pt^{IV}-NCs.

For PPA-Pt^{IV}-NCs, the wide peaks at 1710-1650 cm⁻¹ in the FT-IR spectra were attributed to the asymmetric C=O stretching of ketones and bidentate oxalate from PPA-Pt^{IV}-COOH, and the peak at ~1400 cm⁻¹ belongs to the C-H bending of alkene from PPA. For PEG_{3k}/PPA-Pt^{IV}-NCs, the C-O-C stretching peak was observed at around 1220 cm⁻¹. For ERY₁-PEG_{3k}/PPA-Pt^{IV}-NCs, the characteristic transmittance peaks in FT-IR at 1680 cm⁻¹ (amide, carbonyl stretching), 1541 cm⁻¹ (N-H in-plane bending), and 1390 cm⁻¹ (amide, C-N stretching)¹⁵ confirmed the conjugation of ERY₁ peptide to the nanocomplexes.

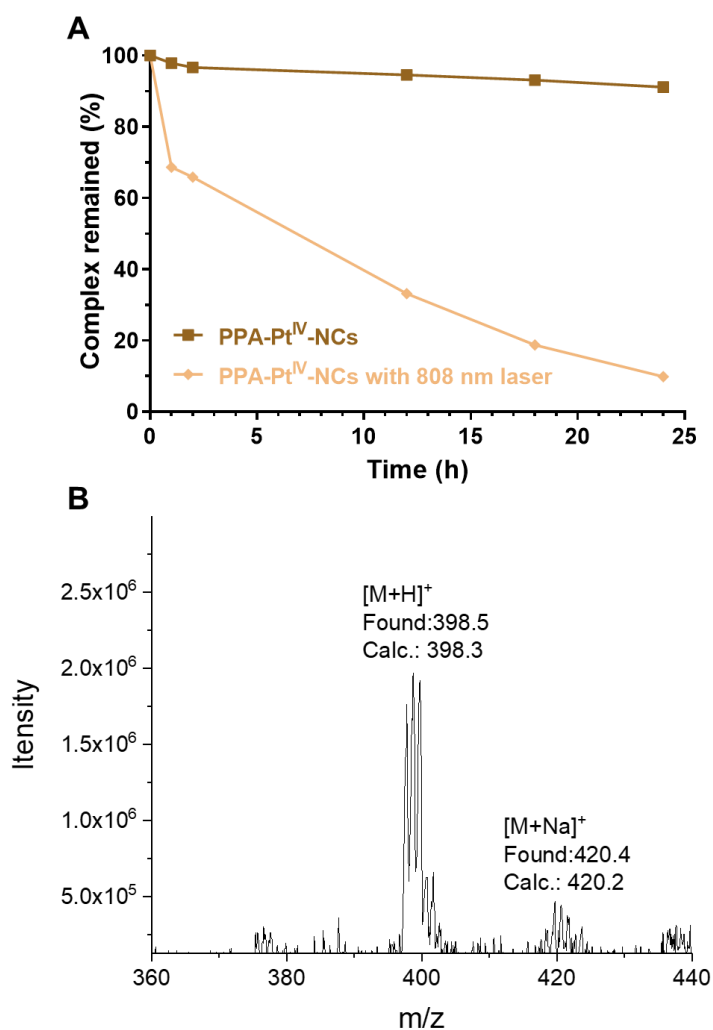


Fig. S12 Release of Pt from PPA-Pt^{IV}-NCs (0.1 mg/mL) **A**) with or without irradiation in PBS containing 0.5 mM ascorbate (pH 7.4). **B**) The release of oxaliplatin after irradiation was confirmed by electrospray ionization mass spectrometry (ESI-MS).

Without irradiation, our nanocomplex was quite stable, and less than 10% Pt was released within 24 h even in the buffer containing ascorbate. Upon irradiation at 808 nm, however, the Pt released more quickly and significantly; 90.2% released after 24 h in PBS containing ascorbate.

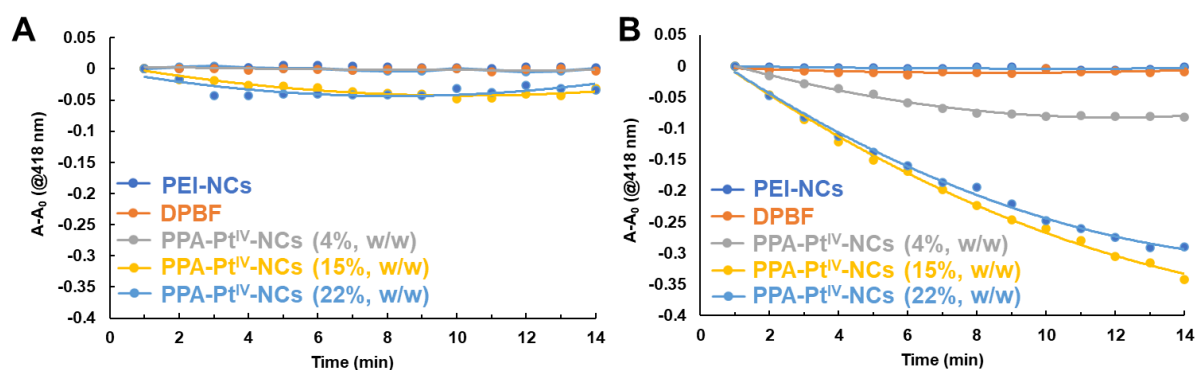


Fig. S13 Generation of $^1\text{O}_2$ through DPBF assay. $^1\text{O}_2$ generated by PPA-Pt^{IV}-NCs in three different loading capacities (4%, 15%, and 22%) **A**) without 808 nm NIR irradiation and **B**) with 808 nm NIR irradiation.

These data also evidence the generation of $^1\text{O}_2$ as the result of efficient energy transfer from NCs to the PPA moiety in the nanocomplex, which is further confirmed by quenching of the red emission band at 670 nm emitted from NCs after conjugation with our Pt(IV) prodrug (Figure 1B).

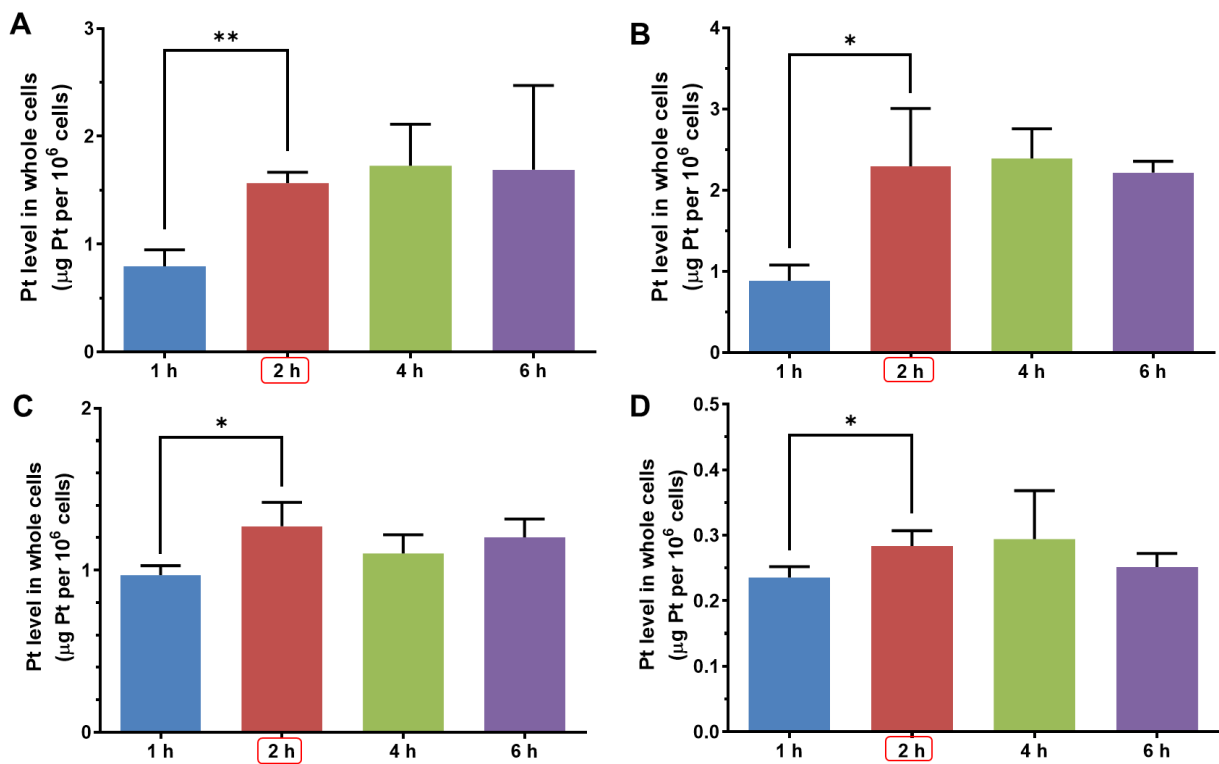


Fig. S14 Time-dependent cellular accumulation of Pt in various cell lines after treated with PPA-Pt^{IV}-NCs (0.1 mg/mL NCs) for 1, 2, 4, and 6 h. The cell lines for the test are **A)** 4T1 cells, **B)** MCF-7 cells, **C)** A2780 cells, and **D)** A2780cisR cells. All treated cells were incubated in the dark and harvested after each time point to test Pt levels. Mean \pm SD; n = 3. *, $p < 0.05$; **, $p < 0.01$.

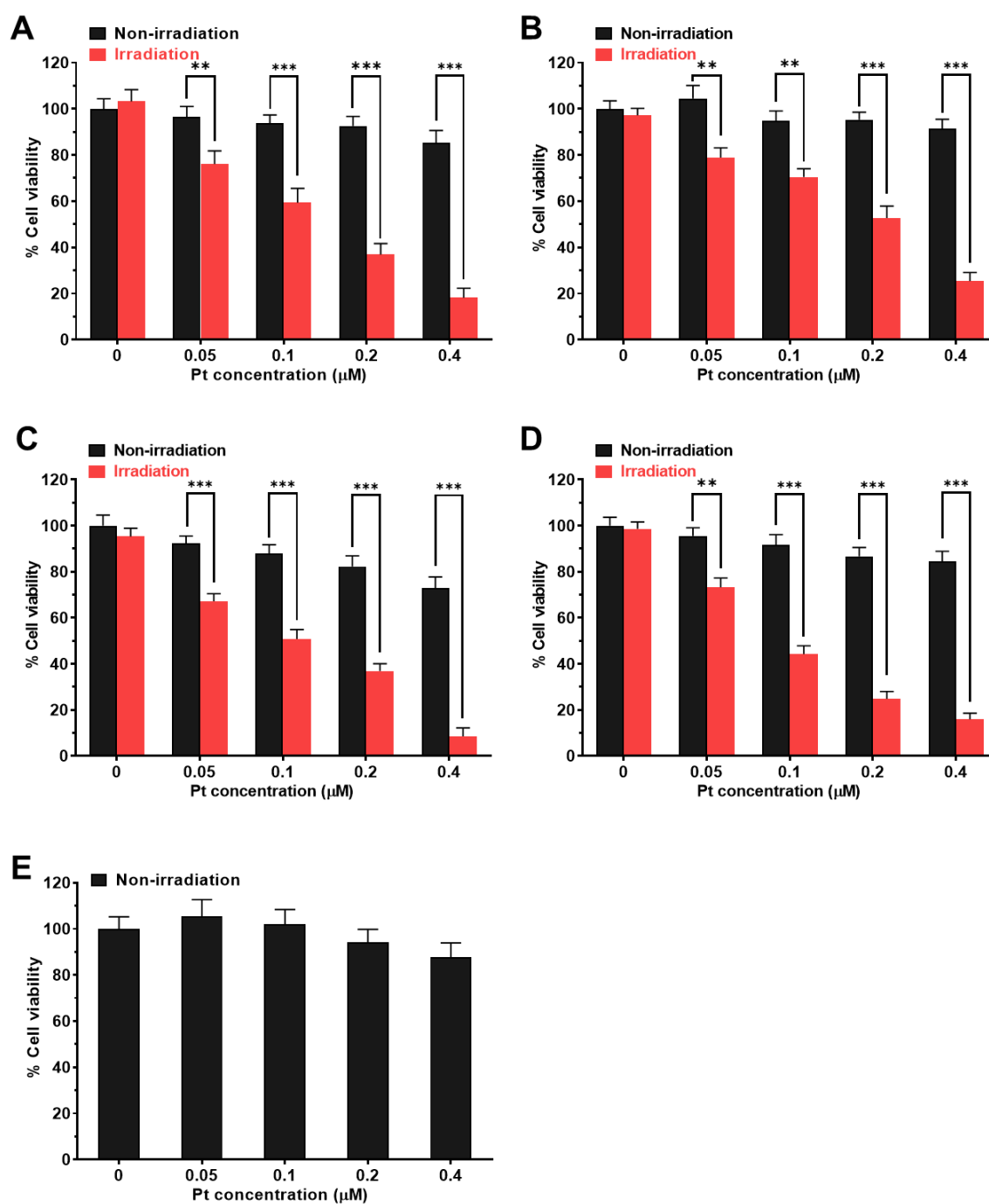


Fig. S15 Phototoxicity of PPA-Pt^{IV}-COOH in **A**) 4T1, **B**) MCF-7, **C**) A2780, **D**) A2780cisR, and **E**) MRC-5 cells with or without 660 nm irradiation. In this assay, the concentrations of Pt were 0.05, 0.1, 0.2, and 0.4 μM , which were the same as those in 0.25, 0.5, 1, and 2 $\mu\text{g}/\text{mL}$ of PPA-Pt^{IV}-NCs (22%, w/w), respectively. The cells were treated with different concentrations of PPA-Pt^{IV}-COOH for 2 h, followed by irradiation at 660 nm (100 mW/cm^2 , 5 min/well) or kept in the dark. The culture medium containing complexes were subsequently replaced by fresh medium and cultured for another 48 h. The cell viabilities of untreated cells (0 μM) without irradiation were set as 100% for calculation. Mean \pm SD; **, $p < 0.01$; ***, $p < 0.001$.

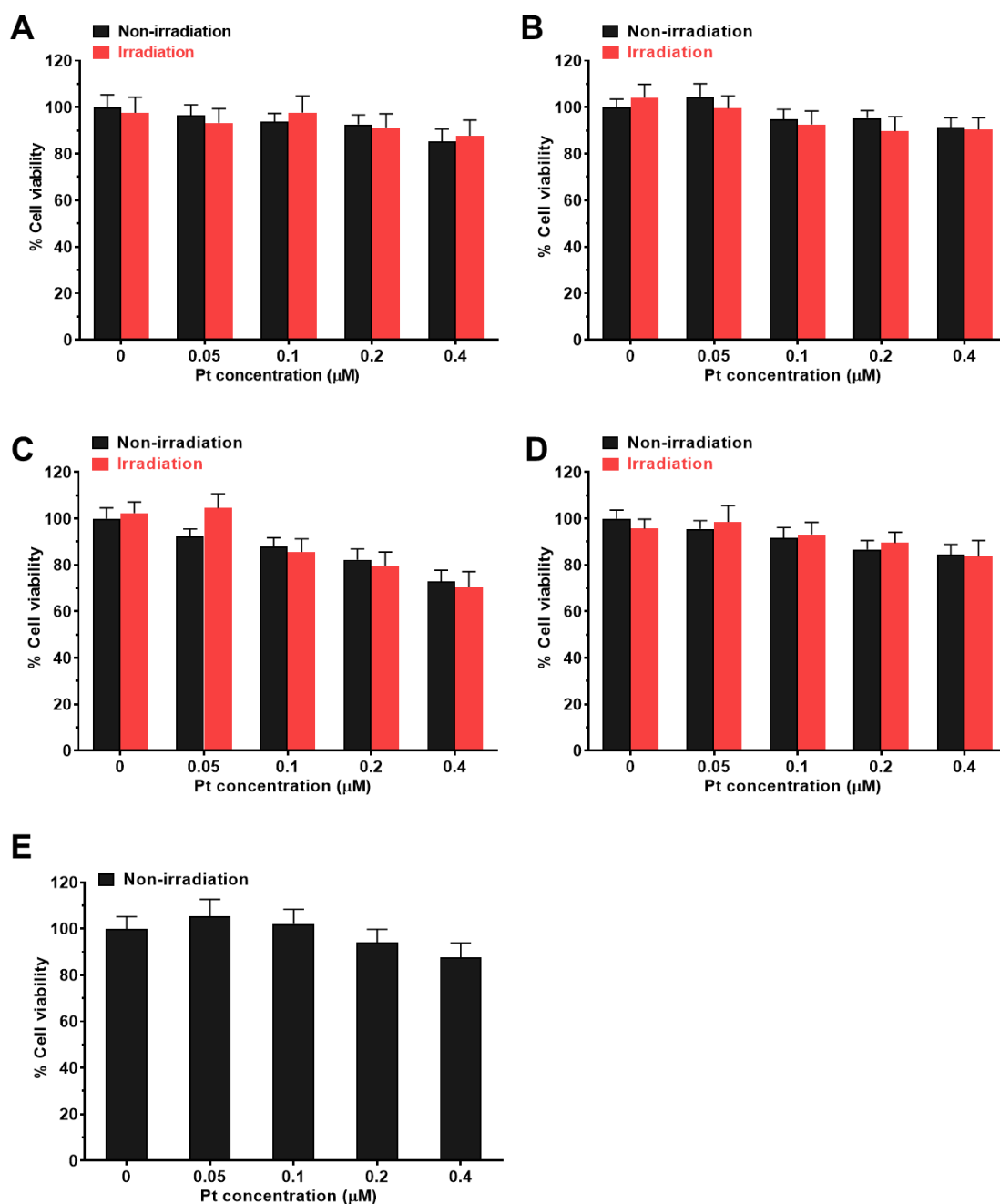


Fig. S16 Phototoxicity of PPA-Pt^{IV}-COOH in **A**) 4T1, **B**) MCF-7, **C**) A2780, **D**) A2780cisR, and **E**) MRC-5 cells with or without 808 nm irradiation. In this assay, the concentrations of Pt were 0.05, 0.1, 0.2, and 0.4 μM , which were the same as those in 0.25, 0.5, 1, and 2 $\mu\text{g}/\text{mL}$ of PPA-Pt^{IV}-NCs (22%, w/w), respectively. The cells were treated with different concentrations of PPA-Pt^{IV}-COOH for 2 h, followed by irradiation at 808 nm (0.5 W/cm², 5 min/well) or kept in the dark. The culture medium containing complexes were subsequently replaced by fresh medium and cultured for another 48 h. The cell viabilities of untreated cells (0 μM) without irradiation were set as 100% for calculation. Mean \pm SD; **, $p < 0.01$; ***, $p < 0.001$.

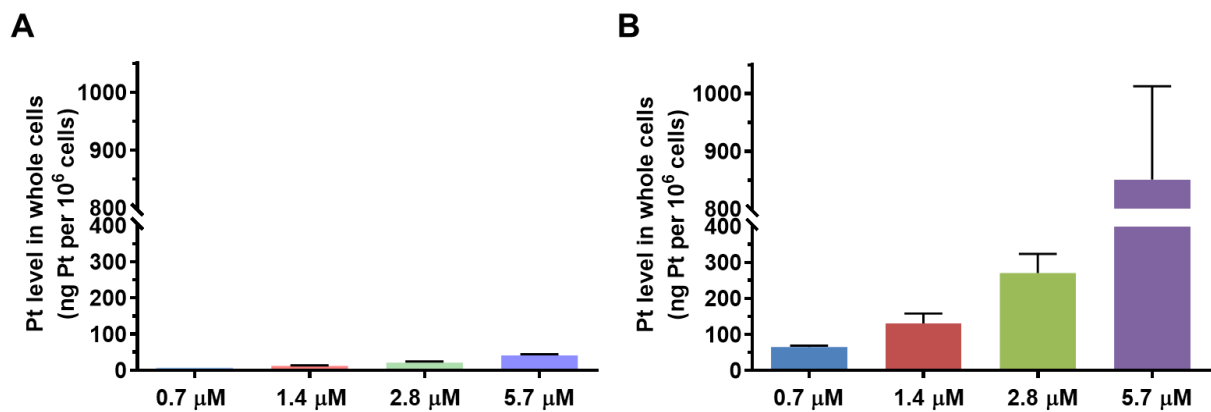


Fig. S17 Concentration-dependent cellular accumulation of Pt in A2780cisR cells. The Pt concentrations of **A)** PPA-Pt^{IV}-COOH and **B)** PPA-Pt^{IV}-NCs are 0.7, 1.4, 2.8, and 5.7 μM . A2780cisR cells were treated for 2 h in the dark. The PPA-Pt^{IV}-NCs showed an increase in the level of Pt by more than 8.9-fold compared to free small molecule PPA-Pt^{IV}-COOH. Mean \pm SD, n = 3.

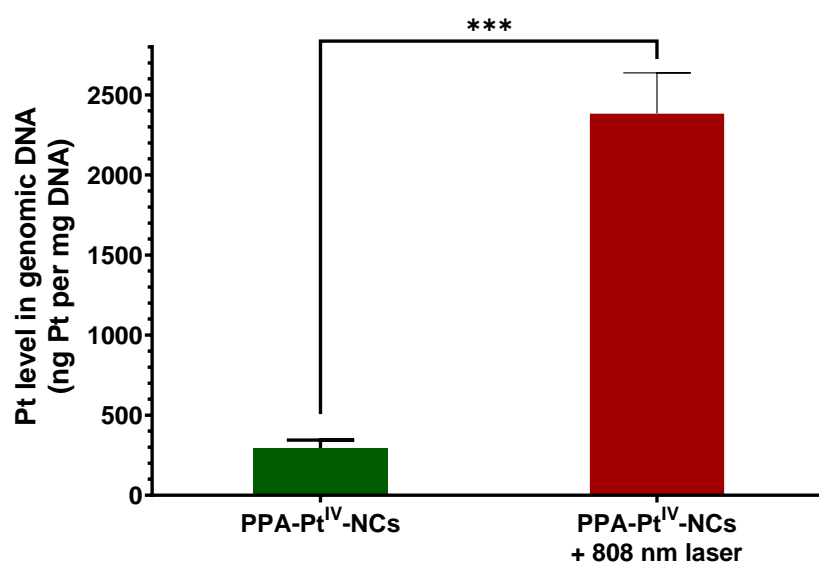


Fig. S18 Pt levels of genomic DNA in A2780cisR cells. The A2780cisR cells were treated with PPA-Pt^{IV}-NCs at a concentration of 0.1 mg/mL NCs. After 2 h of incubation, the cells were treated without/with 808 nm NIR laser (0.5 W/cm², 10 min/dish), and further cultured in fresh medium for another 2 h in the dark. Mean \pm SD; ***, $p < 0.001$.

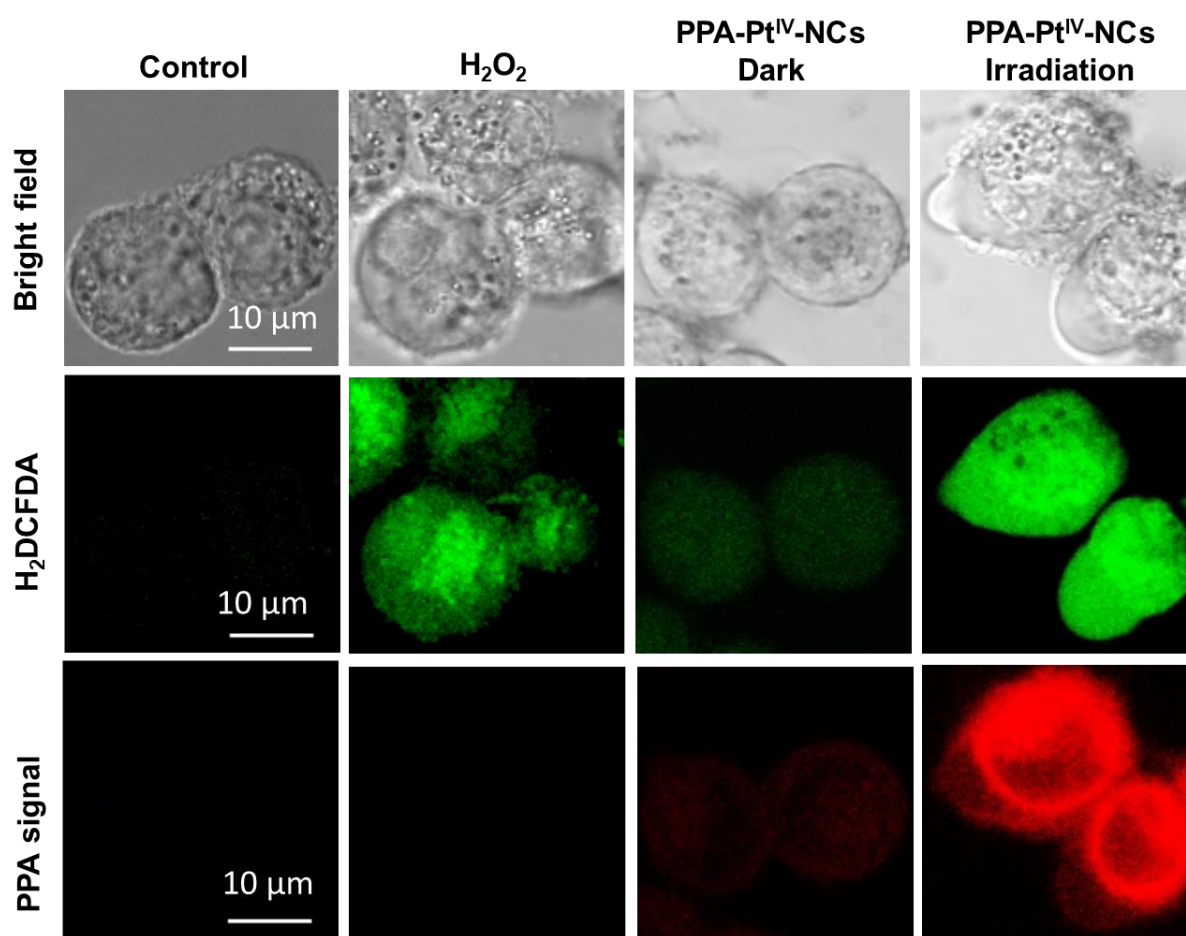


Fig. S19 Confocal images of H₂DCFDA-stained HeLa cells treated with 3 mM H₂O₂ for 15 min or 100 μg·mL⁻¹ PPA-Pt^{IV}-NCs for 1 h with or without 808 nm laser irradiation afterward. Scale bars are 10 μm for the images.

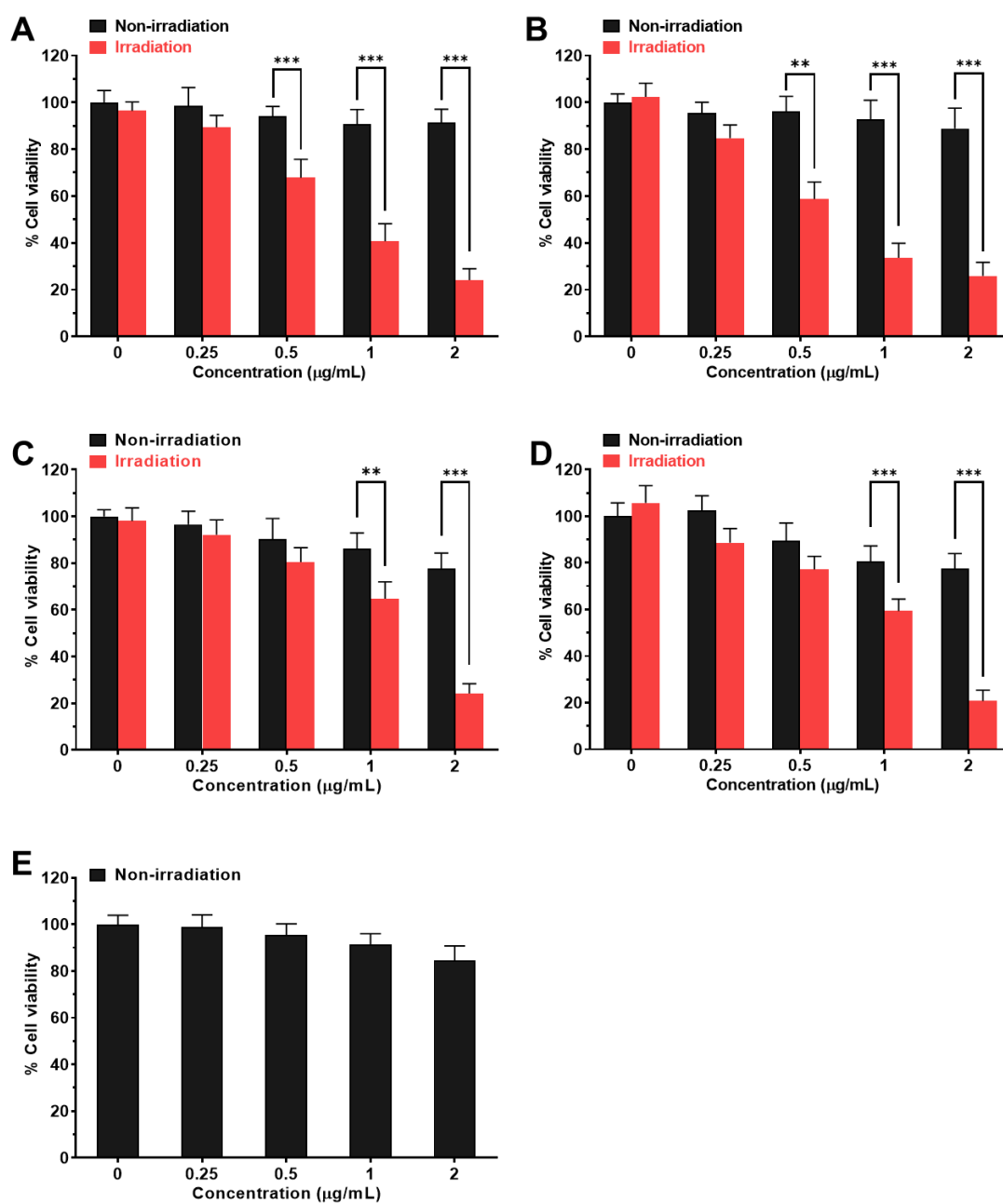


Fig. S20 Phototoxicity of ERY₁-PEG_{3k}/PPA-Pt^{IV}-NCs in **A)** 4T1, **B)** MCF-7, **C)** A2780, **D)** A2780cisR, and **E)** MRC-5 cells with or without 808 nm irradiation. The cells were treated with different concentrations of ERY₁-PEG_{3k}/PPA-Pt^{IV}-NCs for 2 h, followed by irradiation at 808 nm (0.5 W/cm², 5 min/well) or kept in the dark. The culture medium containing nanocomplexes were subsequently replaced by fresh medium and cultured for another 48 h. The cell viabilities of untreated cells (0 µM) without irradiation were set as 100% for calculation. Mean ± SD; **, $p < 0.01$; ***, $p < 0.001$.

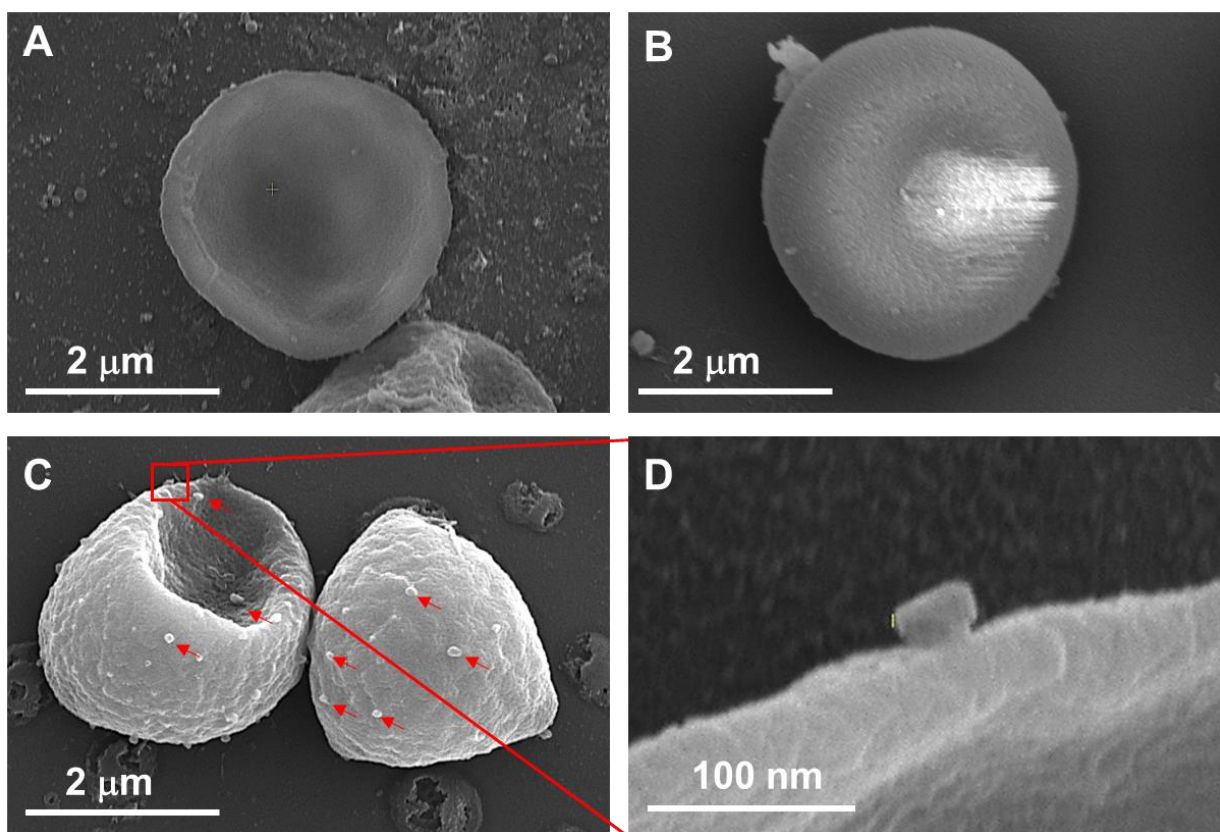


Fig. S21 SEM images of erythrocytes incubated with **A)** 5 mg/mL BSA as control, **B)** PEG_{3k}/PPA-Pt^{IV}-NCs, and **C)** ERY₁-PEG_{3k}/PPA-Pt^{IV}-NCs overnight at 4 °C in the dark. The attached nanoprodruge on the erythrocytes are indicated with red arrows and magnified in **D)**. Scale bars are 2 μm for the images **A-C**, and 100 nm for image **D**.

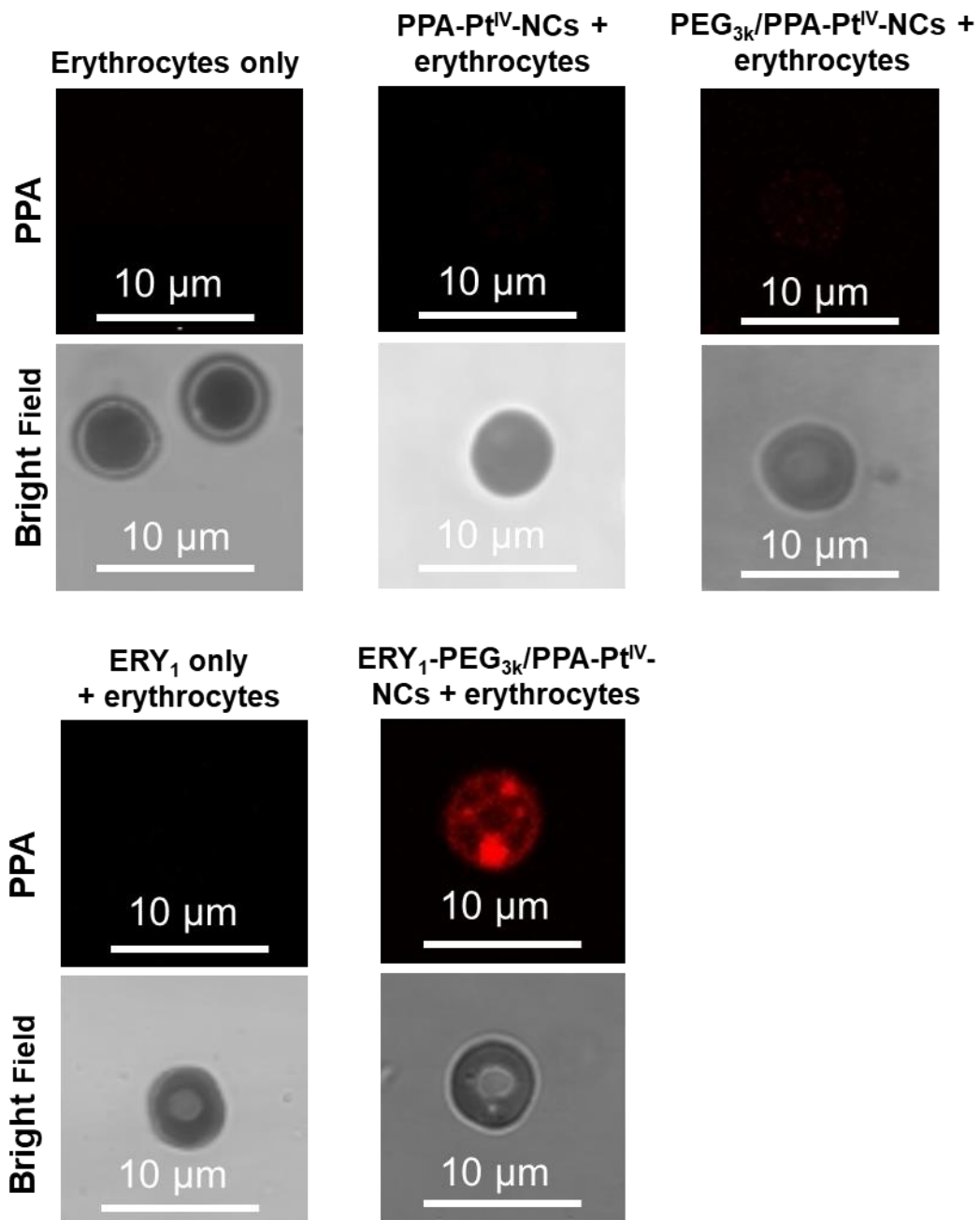


Fig. S22 Confocal fluorescence microscopy images of erythrocytes incubated with various complexes overnight at 4 °C in the dark. Scale bars are 10 μm for the images.

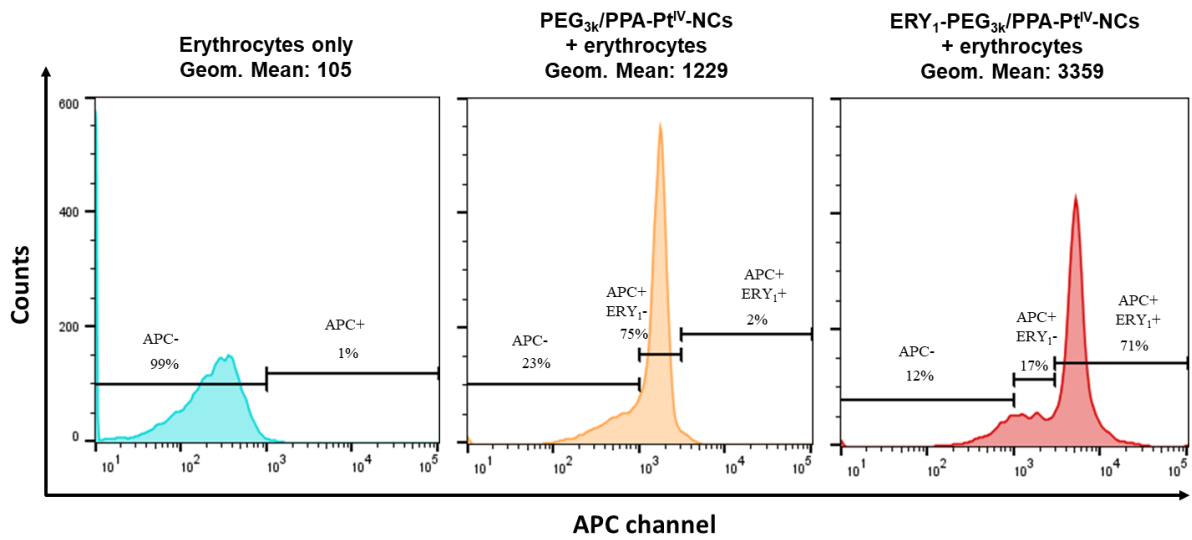


Fig. S23 A quantitative analysis of fluorescence histogram by flow cytometry depicting the erythrocytes and after incubation with indicated complexes (PEG_{3k}/PPA-Pt^{IV}-NCs and ERY₁-PEG_{3k}/PPA-Pt^{IV}-NCs). The APC channel was selected to detect the PPA signal with Ex = 638 nm, Em = 660 nm.

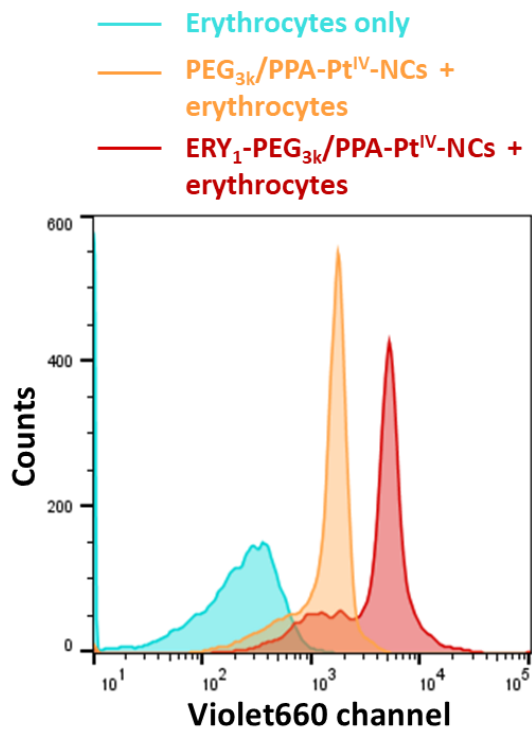


Fig. S24 Merged flow cytometry depicting the fluorescence intensity of erythrocytes incubated with indicated complexes. The APC channel was selected to detect the PPA signal with Ex = 638 nm, Em = 660 nm.

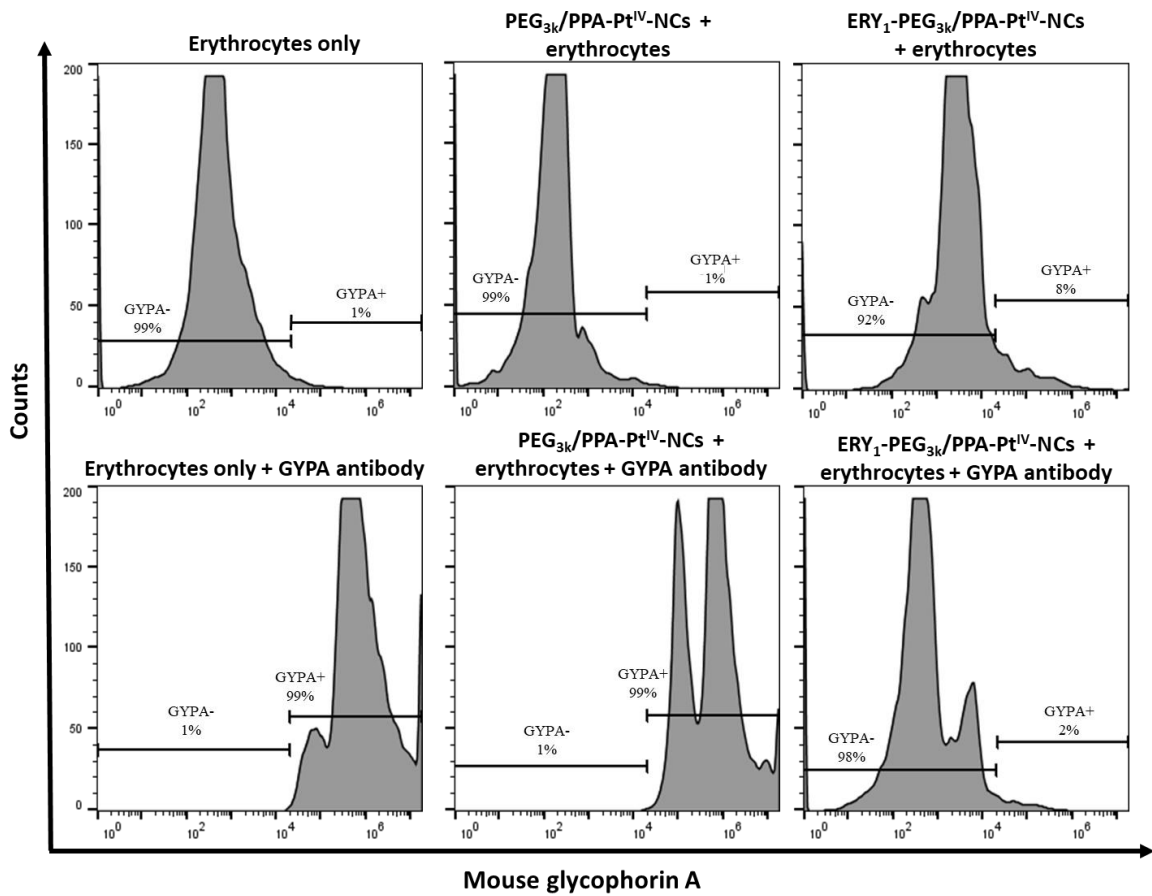


Fig. S25 A quantitative analysis of fluorescence histogram by flow cytometry depicting the glycoprotein A (GYPA) on erythrocytes and after incubation with indicated complexes (PEG_{3k}/PPA-Pt^{IV}-NCs, and ERY₁-PEG_{3k}/PPA-Pt^{IV}-NCs). The Alexa 488 channel was selected to detect the GYPA signal.

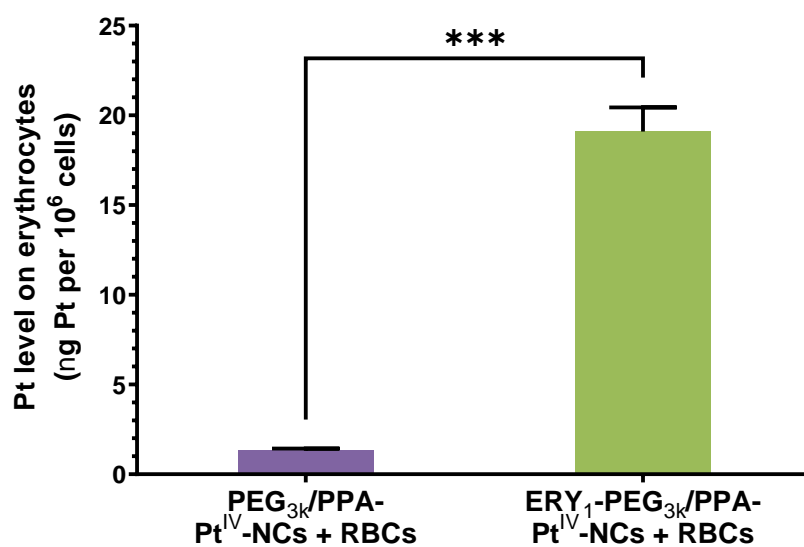


Fig. S26 Pt levels on erythrocytes. The erythrocytes were treated with PEG_{3k}/PPA-Pt^{IV}-NCs and ERY₁-PEG_{3k}/PPA-Pt^{IV}-NCs at a concentration of 0.1 mg/mL NCs. After washed twice with PBS (pH 7.4), the erythrocytes were collected and digested with acid for ICP-OES. Mean \pm SD; ***, $p < 0.001$.

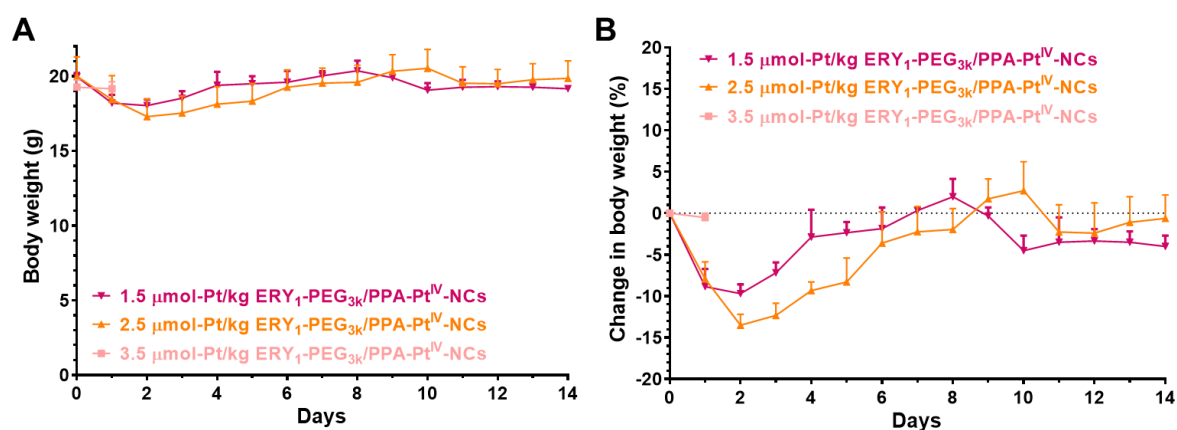


Fig. S27 The change of body weight of BALB/c mice upon treatment with various doses of ERY₁-PEG_{3k}/PPA-Pt^{IV}-NCs (*i.v.* injection, single dose on Day 0). **A)** The absolute body weight change and **B)** the relative change of body weight after *i.v.* injection during the monitor period. 0.9% saline is the vehicle in the whole experiment. Mean \pm SD; n = 3.

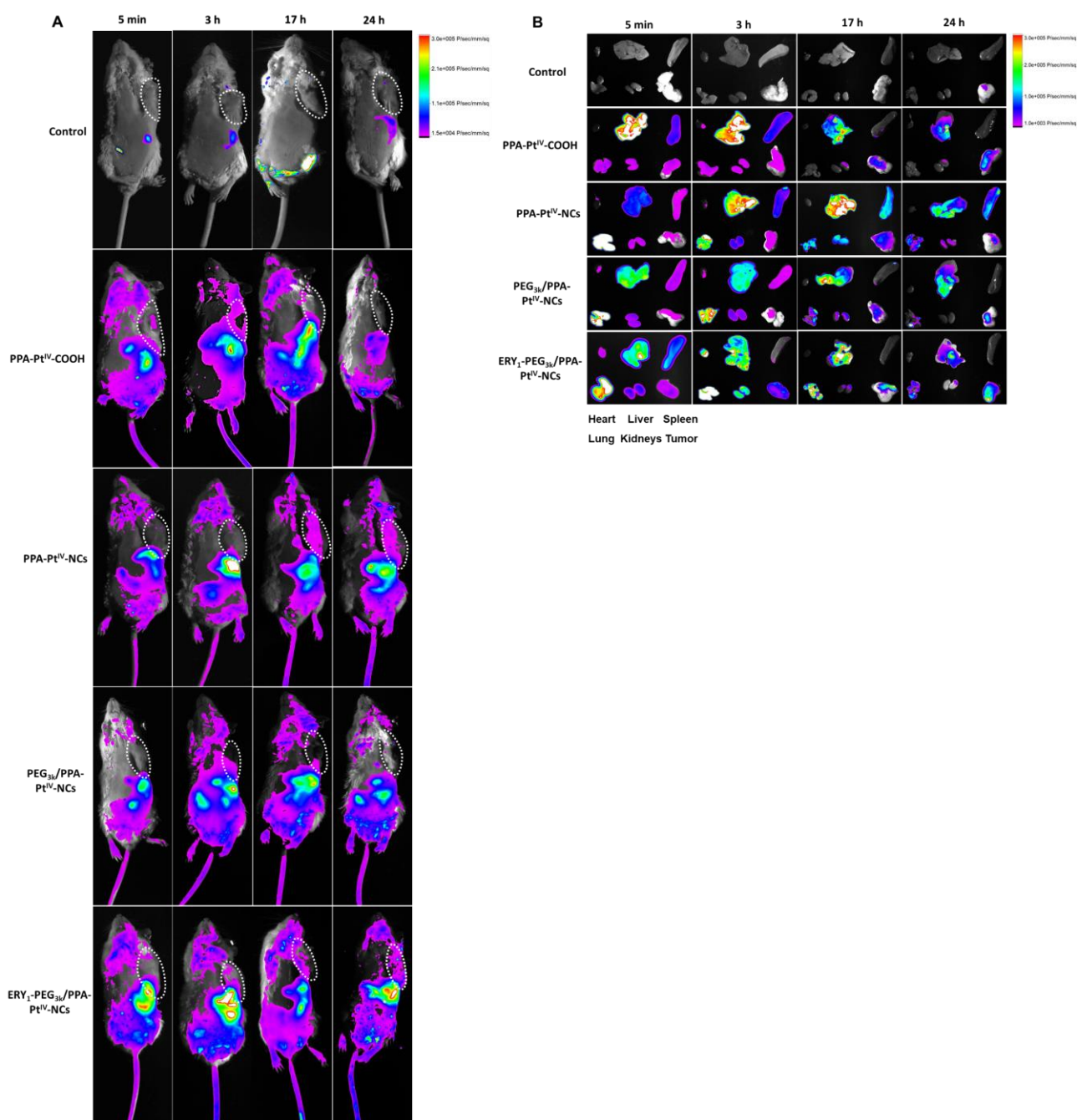


Fig. S28 *In vivo* fluorescence imaging of **A)** 4T1 tumor-bearing BALB/c mice and **B)** corresponding organs after intravenously (*i.v.*) injected with various complexes at 5 min, 3 h, 17 h, and 24 h post-injection. The organs in each figure are: first line, heart, liver, spleen; second line, lung, kidney, tumor. The injection dose is 1.3 mg-Pt/kg. The mice in the control group were injected with 0.9% saline. Ex = 650 nm, Em = 670-750 nm.

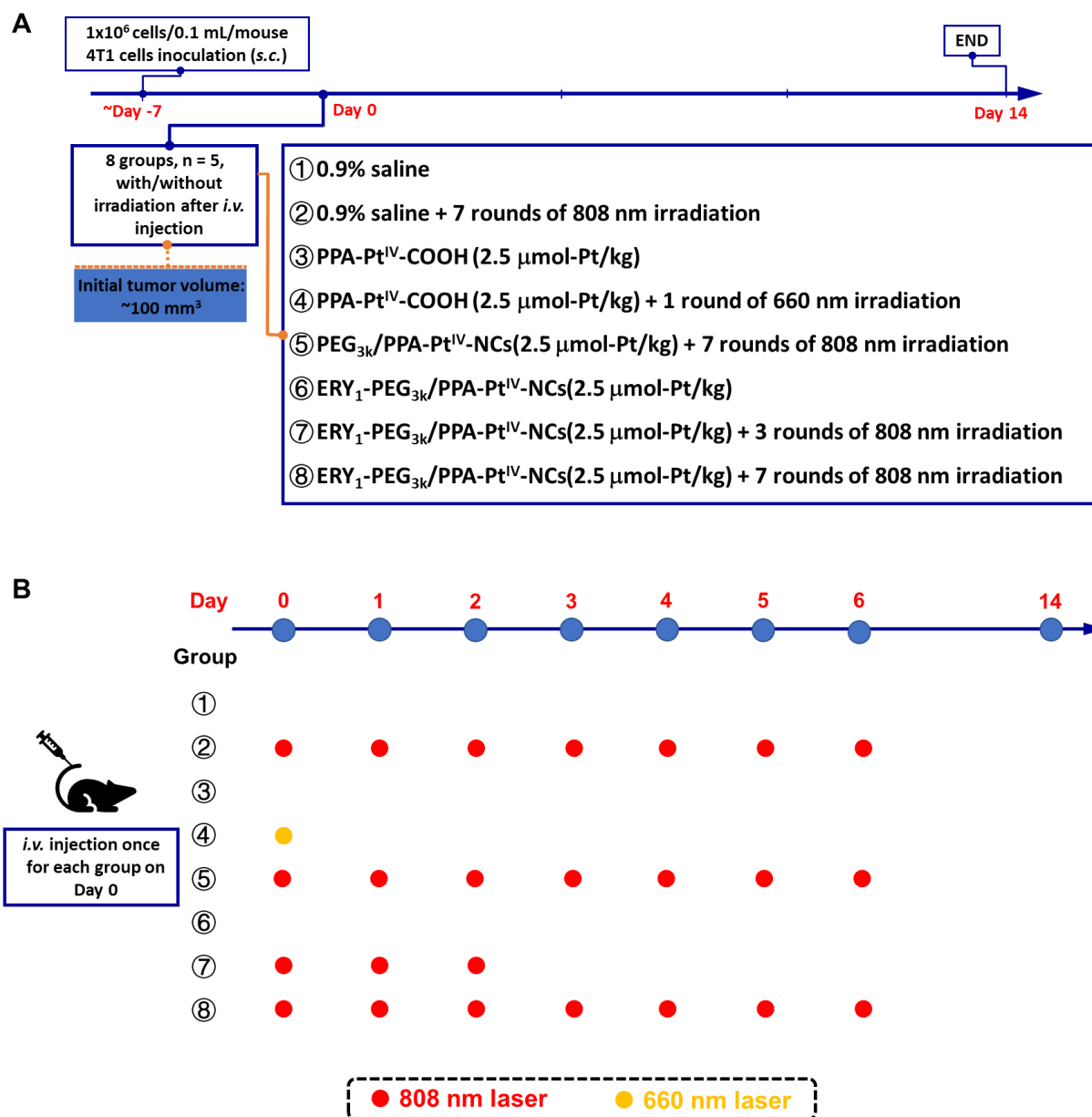


Fig. S29 The schedule of *in vivo* experiment to evaluate the anticancer activity in the 4T1 xenograft model. **A)** The schedule for anticancer evaluation; **B)** detailed irradiation plan for each group. 4T1 cells (1×10^6 cell/0.1 mL/mouse) were subcutaneously (s.c.) inoculated in BALB/c mice at Day -7 to establish the xenograft mouse model (8 groups, n = 5). When the tumor masses achieved a volume around 100 mm^3 , the treatment started at Day 0. The mice received complexes indicated above. The complexes were intravenously (*i.v.*) injected only once on Day 0 and treated with/without irradiation. Irradiation conditions: 660 nm laser (100 mW/cm^2) for 10 min per mouse, 808 nm laser (0.5 W/cm^2) for 30 min (5 min irradiation with 5 min interval) per mouse. The detail was listed in the method part.

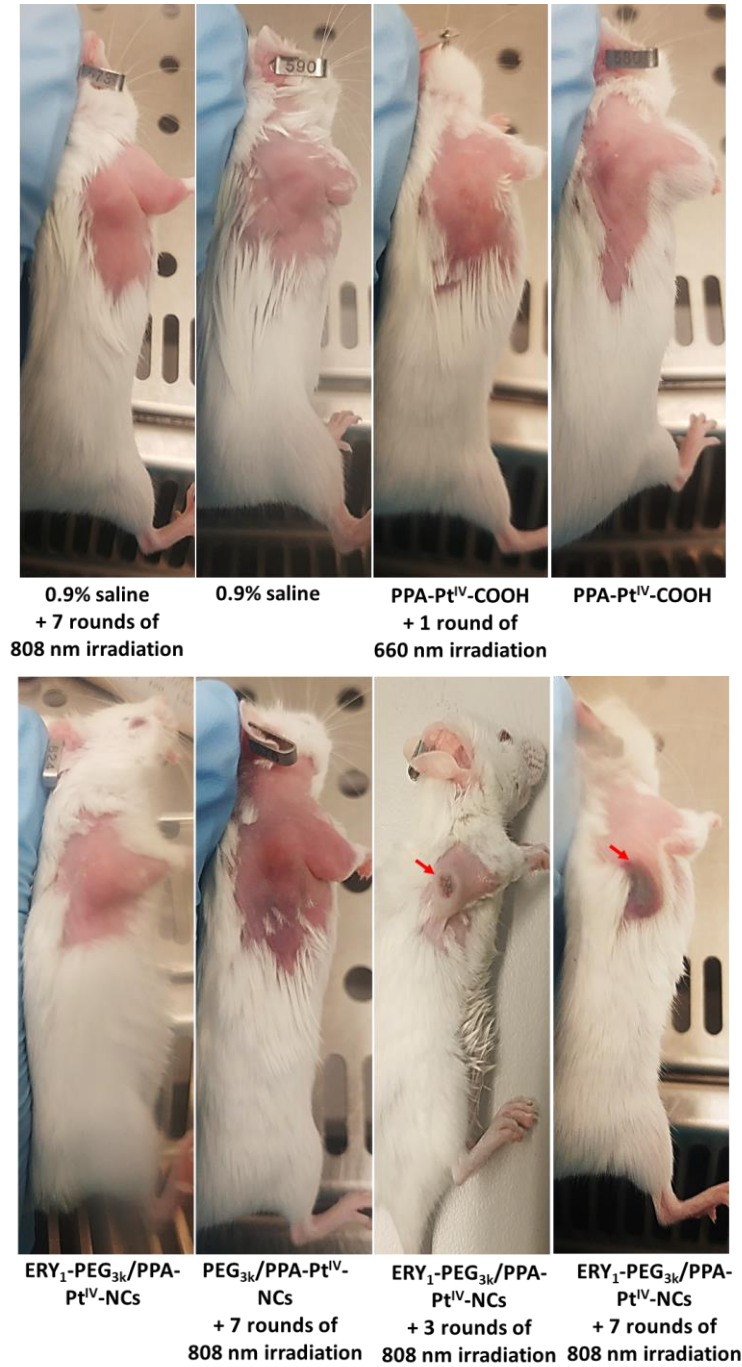


Fig. S30 The digital photos on Day 1 of the 4T1 xenograft model after different treatments. Irradiation conditions: 660 nm laser (100 mW/cm²) for 10 min per mouse, 808 nm laser (0.5 W/cm²) for 30 min (5 min irradiation with 5 min interval) per mouse. The strong antitumor effect of the nanoprodrug was indicated with red arrows.

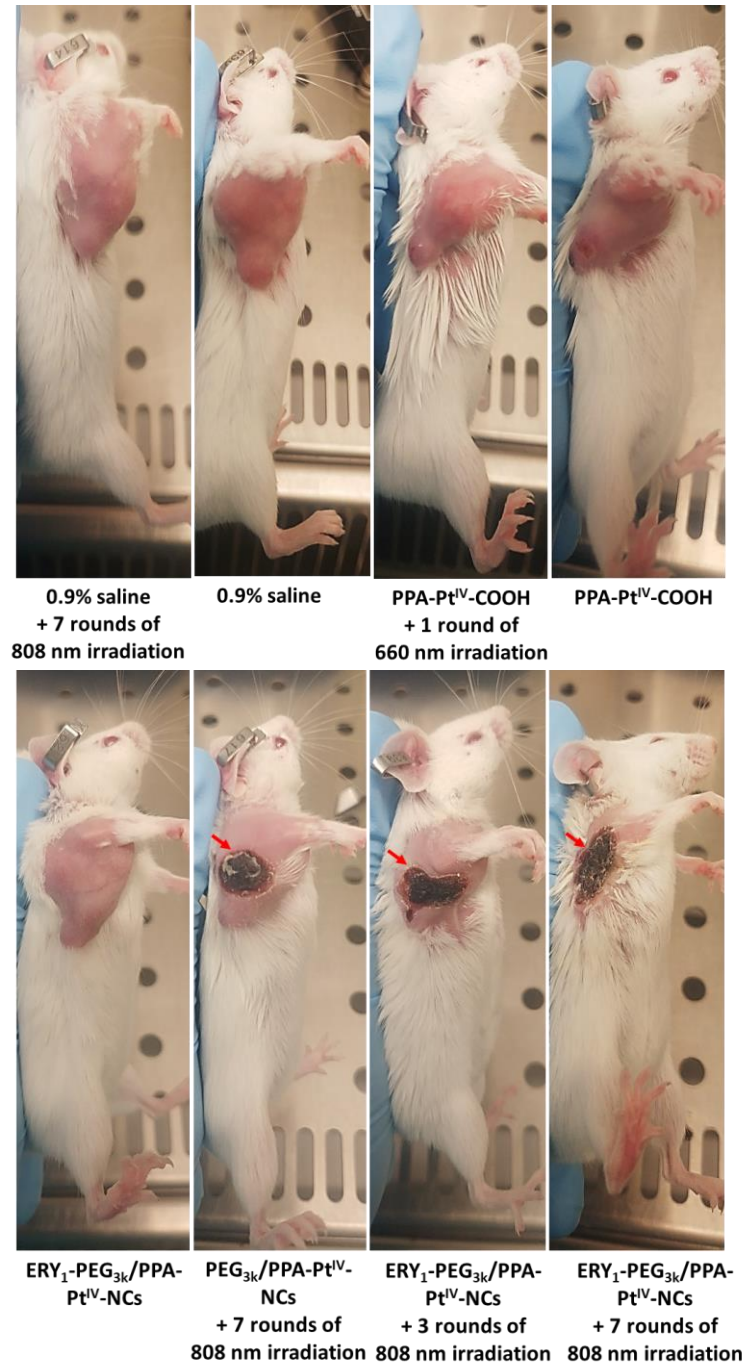


Fig. S31 The digital photos on Day 14 of the 4T1 xenograft model after different treatments. Irradiation conditions: 660 nm laser (100 mW/cm²) for 10 min per mouse, 808 nm laser (0.5 W/cm²) for 30 min (5 min irradiation with 5 min interval) per mouse. The strong antitumor effect of the nanoprodruge was indicated with red arrows.

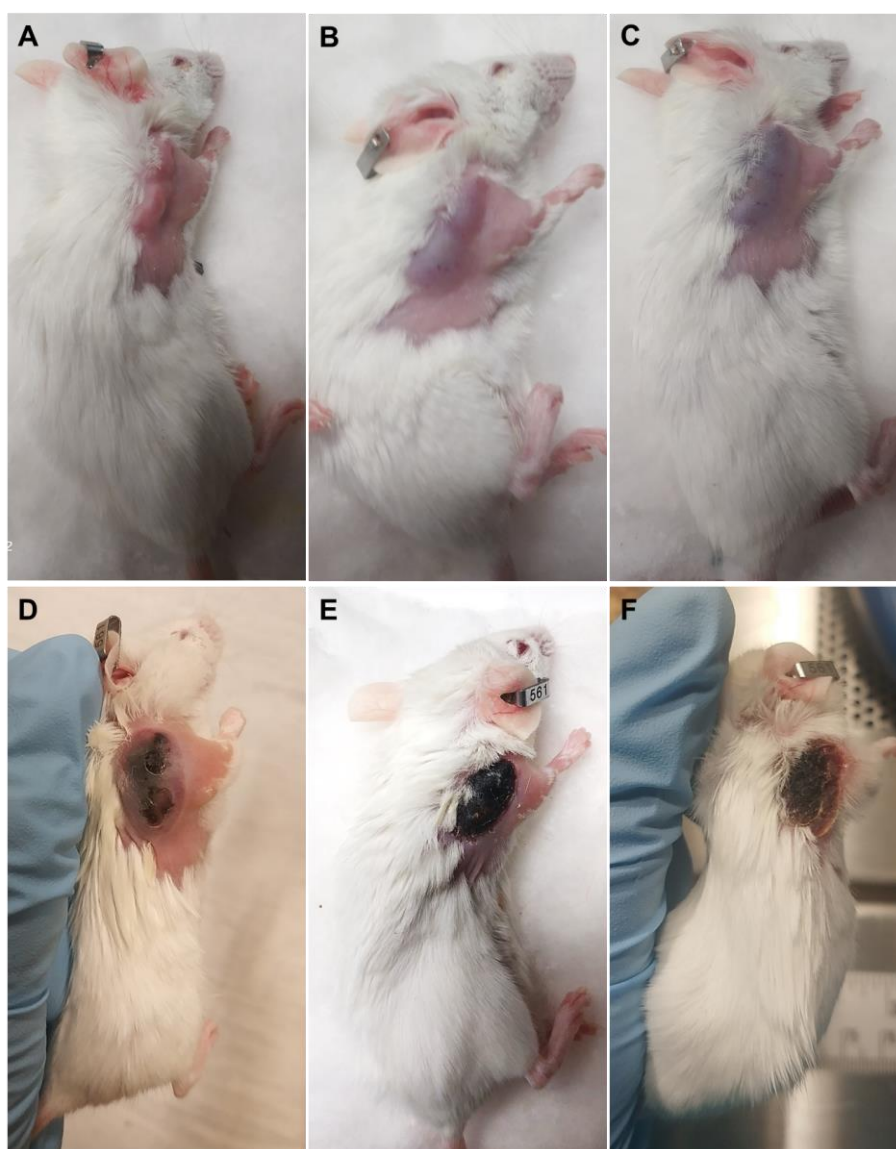


Fig. S32 The digital photos of the same mouse from ERY₁-PEG_{3k}/PPA-Pt^{IV}-NCs group with 7 times of 808 nm irradiation. The images were acquired **A)** before irradiation, Day 0; **B)** 15 min post-irradiation, Day 0; **C)** 30 min post-irradiation, Day 0; **D)** after irradiation for twice, Day 2; **E)** after three rounds of irradiation, Day 3; and **F)** after 7 rounds of irradiation, Day 7. Irradiation conditions: 660 nm laser (100 mW/cm²) for 10 min per mouse, 808 nm laser (0.5 W/cm²) for 30 min (5 min irradiation with 5 min interval) per mouse.

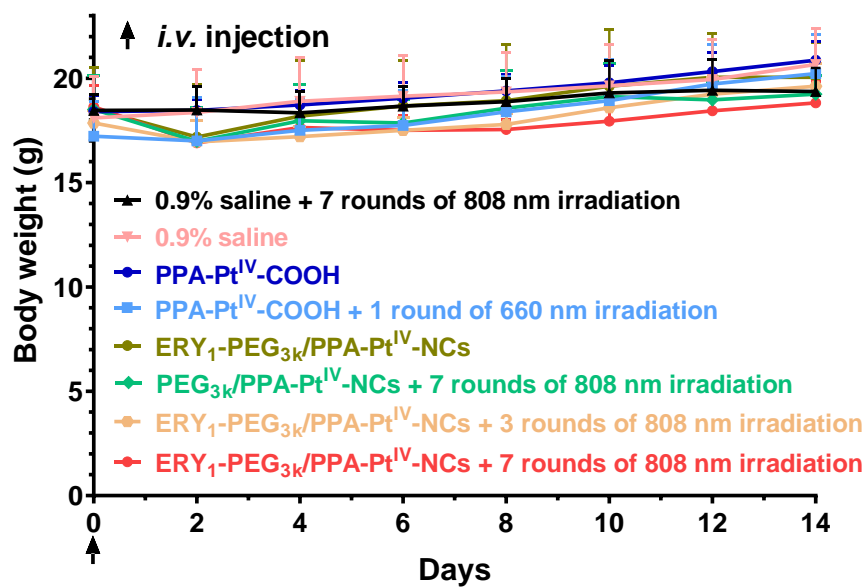


Fig. S33 The change of body weight of the 4T1 xenograft model with different treatments. The indicated complexes were intravenously (*i.v.*) injected only once on Day 0 and treated with/without irradiation. Irradiation conditions: 660 nm laser (100 mW/cm²) for 10 min per mouse, 808 nm laser (0.5 W/cm²) for 30 min (5 min irradiation with 5 min interval) per mouse. The detail was listed in the method part. Mean ± SD, n = 5.

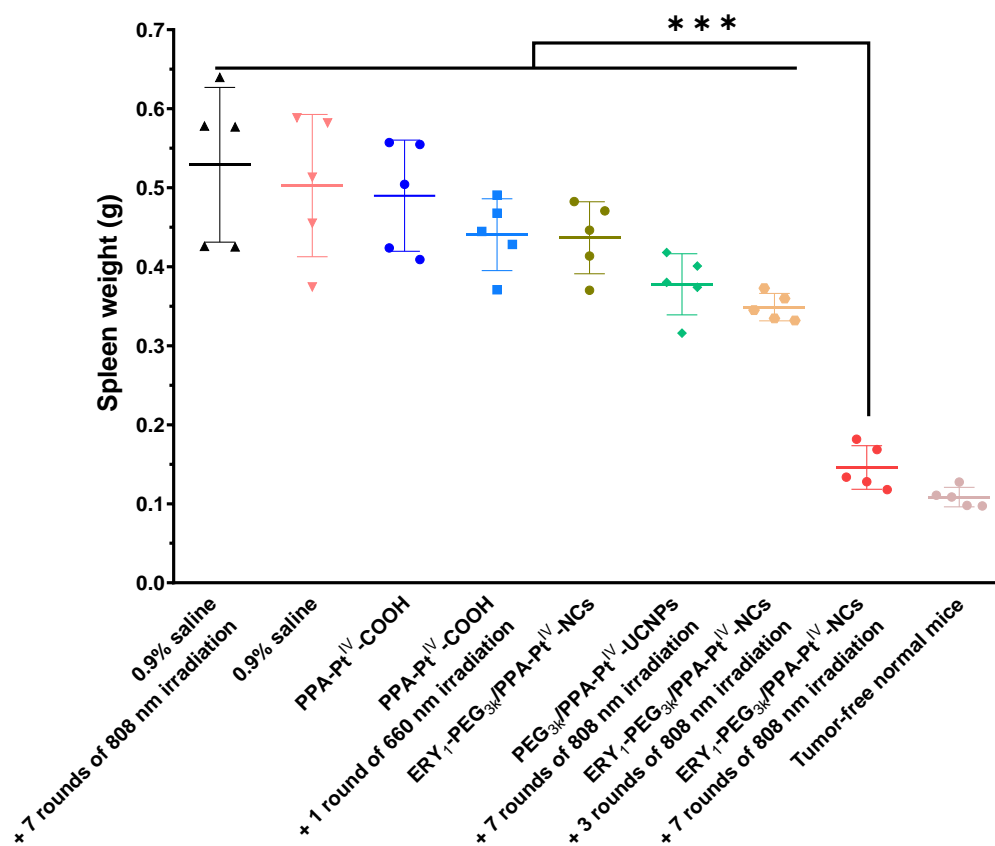


Fig. S34 Spleen weights of different groups of 4T1 xenograft model after the experiment terminated. The indicated complexes were intravenously (*i.v.*) injected only once on Day 0 and treated with/without irradiation. Irradiation conditions: 660 nm laser (100 mW/cm²) for 10 min per mouse, 808 nm laser (0.5 W/cm²) for 30 min (5 min irradiation with 5 min interval) per mouse. The detail was listed in the method part. Mean \pm SD, n = 5. ***, $p < 0.001$. Student's t-Test.

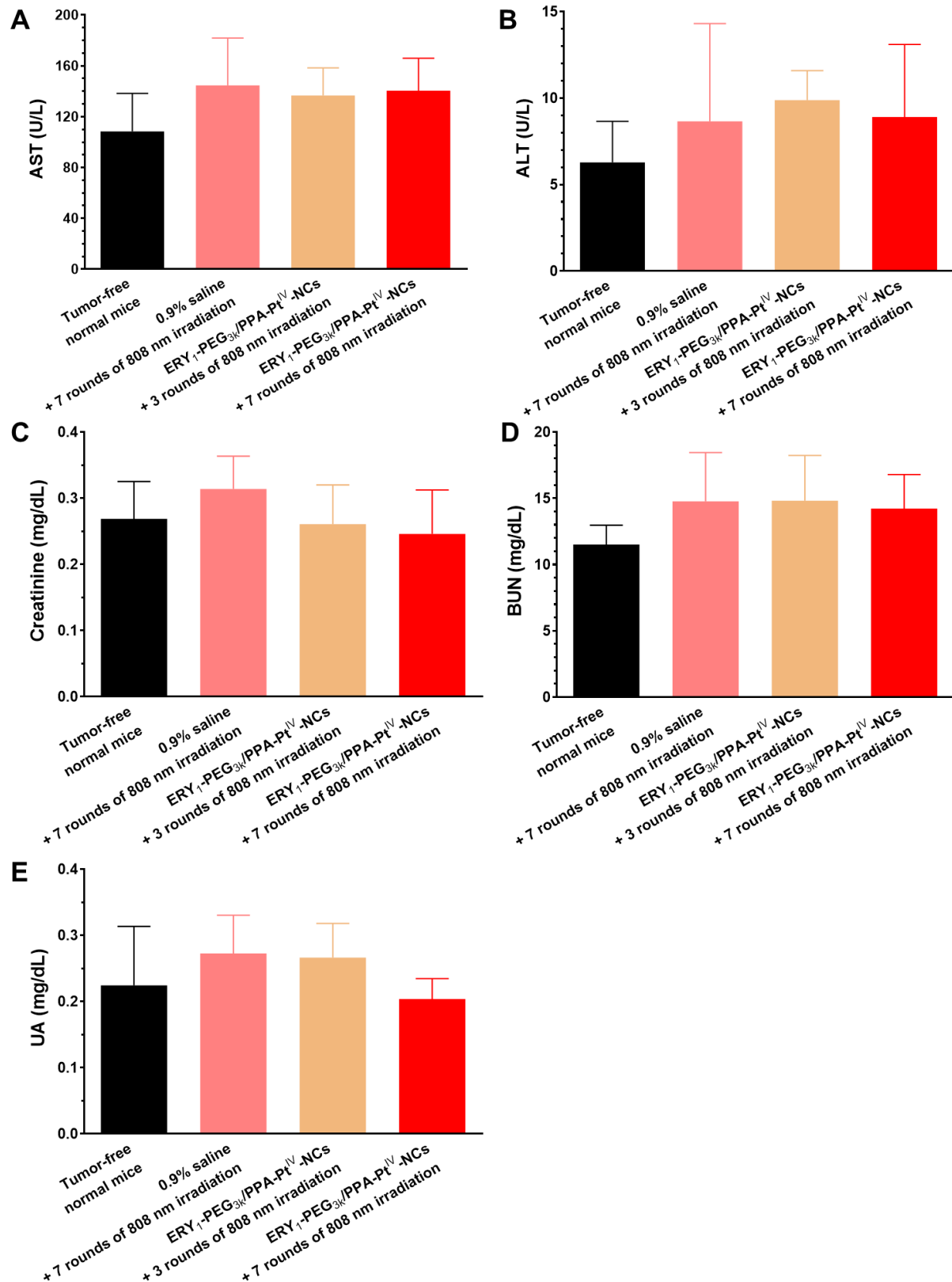


Fig. S35 Hematology study of blood plasma from 4T1 xenograft model after experiment terminated (Day 14) with **A**) aspartate transaminase (AST), **B**) alanine aminotransferase (ALT), **C**) creatinine, **D**) blood urea nitrogen (BUN), and **E**) uric acid (UA). All the biochemical parameters are in the normal range. Mean \pm SD, n = 5.

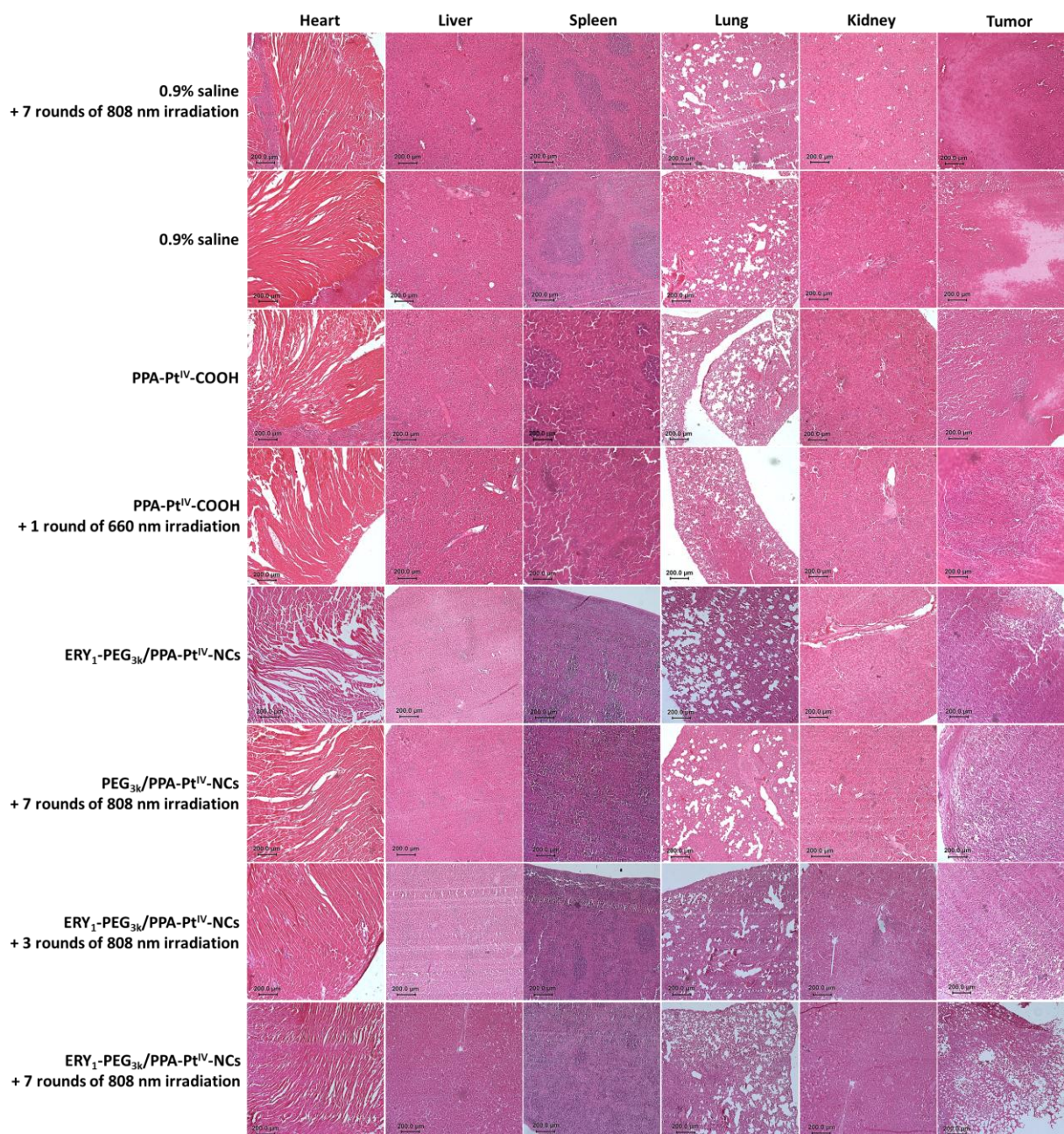


Fig. 36 H&E staining of the organs and tumors at the end of antitumor studies. Scale bars are 200 μm for the images.

Table S1. Diameter and zeta potential of PEI-NCs and the various nanocomplexes containing Pt(IV) prodrug.

Mean \pm SD, n = 3.

Sample	Intensity hydrodynamic size (d. nm)	Zeta potential (mV)
PEI-NCs	91.9 \pm 20.4	37.9 \pm 0.2
PPA-Pt ^{IV} -NCs (4%, w/w)	119.7 \pm 6.2	35.1 \pm 2.1
PPA-Pt ^{IV} -NCs (15%, w/w)	129.2 \pm 9.5	28.2 \pm 1.0
PPA-Pt ^{IV} -NCs (22%, w/w)	134.7 \pm 2.7	20.9 \pm 2.0
PEG _{3k} /PPA-Pt ^{IV} -NCs	147.1 \pm 3.2	-1.2 \pm 1.7
ERY ₁ -PEG _{3k} /PPA-Pt ^{IV} -NCs	156.8 \pm 22.0	-2.1 \pm 4.0

After conjugated with various ratios of PPA-Pt^{IV}-COOH on NCs, the decrease of zeta potential was observed, which was ascribed to the increased loading amount of negatively charged Pt(IV) prodrug, neutralizing the positively charged PEI-NCs. The average hydrodynamic size of PEI-NCs was 91.9 \pm 20.4 nm, and the value steadily increased to 119.7 \pm 6.2, 129.2 \pm 6.2, and 134.7 \pm 2.7 nm for PPA-Pt^{IV}-NCs with LC% of 4%, 15%, and 22%, respectively.

The presence of PEG in PEG_{3k}/PPA-Pt^{IV}-NCs was also confirmed by neutralized charge (-1.2 mV).

The ζ potential of ERY₁-PEG_{3k}/PPA-Pt^{IV}-NCs was determined to be -2.1 mV. This slight decrease of ζ potential after functionalization with ERY₁ revealed the successful conjugation due to the different electrical charge of the peptide. Besides, the increase of the hydrodynamic size also suggested the successful conjugation of the peptide on the PEG linker.

Table S2. Calculated pharmacokinetics parameters.

Parameter	Unit	PPA-Pt ^{IV} -COOH	PEG _{3k} /PPA-Pt ^{IV} -NCs	ERY ₁ -PEG _{3k} /PPA-Pt ^{IV} -NCs
t_{1/2}	h	0.79	α : 0.62 β : 1078.90	907.76
AUC	mg/(L*h)	520.7	457.73	452.21
V_d	(μ mol/kg)/(mg/L)	0.57	0.49	0.85
V_{ss}	(μ mol/kg)/(mg/L)	0.57	0.95	0.85

For the curve fits the first-order kinetics elimination for the One-Compartment Open Model: Intravenous Bolus Administration, it assumes that the drug is administered instantly into the body and rapidly distributed through the body, while the drug elimination occurs simultaneously. In this condition, the profile is expressed as $t_{1/2}$.

$t_{1/2}$: half-life ---- the time taken for half the initial dose of medicine administered to be eliminated from the body;

For the curve fits the Two-Compartment Open Model: Intravenous Bolus Administration, it indicates the drug does not equilibrate rapidly as the one-compartment model. The time profile of this condition includes distribution phase and elimination phase which are expressed as $t_{1/2\alpha}$ and $t_{1/2\beta}$, respectively.

$t_{1/2\alpha}$: distribution half-life ---- the amount of time required for the plasma concentration to decline by 50% during the distribution phase;

$t_{1/2\beta}$: elimination half-life ---- the amount of time required for the plasma concentration to decline by 50% during the elimination phase;

AUC: area under the curve ---- the integral of the concentration-time curve after a single dose;

V_d: the apparent volume of distribution during the terminal phase;

V_{ss}: the apparent volume of the plasma compartment.

Supplementary References

1. H. Wen, H. Zhu, X. Chen, T. F. Hung, B. Wang, G. Zhu, S. F. Yu and F. Wang, *Angew. Chem. Int. Ed.*, 2013, **52**, 13419-13423.
2. W. Kong, T. Sun, B. Chen, X. Chen, F. Ai, X. Zhu, M. Li, W. Zhang, G. Zhu and F. Wang, *Inorg. Chem.*, 2017, **56**, 872-877.
3. L.-Q. Xiong, Z.-G. Chen, M.-X. Yu, F.-Y. Li, C. Liu and C.-H. Huang, *Biomaterials*, 2009, **30**, 5592-5600.
4. P. W. Riddles, R. L. Blakeley and B. Zerner, in *Methods Enzymol.*, Academic Press, **1983**, vol. 91, pp. 49-60.
5. P. W. Riddles, R. L. Blakeley and B. Zerner, *Anal. Biochem.*, 1979, **94**, 75-81.
6. S. Parasuraman, R. Raveendran and R. Kesavan, *J. Pharmacol. Pharmacother.*, 2010, **1**, 87-93.
7. R. A. R. Bowen and A. T. Remaley, *Biochem. Med.*, 2014, **24**, 31-44.
8. S. Kontos and J. A. Hubbell, *Mol. Pharm.*, 2010, **7**, 2141-2147.
9. Y. Zhang, M. Huo, J. Zhou and S. Xie, *Comput. Methods Programs Biomed.*, 2010, **99**, 306-314.
10. R. I. Freshney, *Wiley-Liss: Hoboken, NJ, USA*, **2005**.
11. Dissociation of Cells from Primary Tissue. *Thermo Fisher Scientific*, <https://www.thermofisher.com/cn/en/home/references/protocols/cell-culture/primary-cell-protocols/dissociation-of-cells-from-primary-tissue.html>.
12. L. He, T. Nie, X. Xia, T. Liu, Y. Huang, X. Wang and T. Chen, *Adv. Funct. Mater.*, 2019, **29**, 1901240.
13. J. Ogasawara, R. Watanabe-Fukunaga, M. Adachi, A. Matsuzawa, T. Kasugai, Y. Kitamura, N. Itoh, T. Suda and S. Nagata, *Nature*, 1993, **364**, 806-809.
14. S. Dhar, N. Kolishetti, S. J. Lippard and O. C. Farokhzad, *Proc. Natl. Acad. Sci. U.S.A.*, 2011, **108**, 1850-1855.
15. J. Coates, *Encyclopedia of Analytical Chemistry*, John Wiley & Sons Ltd, Chichester, 2000.